Introduction to Tokamak Plasma Control*

Michael L. Walker, Peter De Vries, Federico Felici, and Eugenio Schuster

Abstract— **This paper provides an introduction to the problems of control of plasmas and plasma magnetic-confinement devices known as tokamaks. The basic science of fusion plasmas and objectives of plasma magnetic-confinement technologies are described. In addition to a general overview of plasma control problems, more extensive discussions of three specific classes of problems - control of plasma magneto-hydrodynamic behavior, control of plasma parameter internal distributions, and methods for handling system faults or unexpected loss of control - are provided.**

I. INTRODUCTION

This paper provides an introduction to the problems of plasma control in tokamaks – plasma-confining devices used in magnetic-confinement fusion research. Significant progress has been made in the decades since controlled magnetic fusion was first envisioned as a potential power source, most focused on achieving necessary scientific understanding of fusion plasmas and how best to produce energy-generating fusion reactions within those plasmas. As greater scientific understanding was gained, more attention began to be paid to technological issues associated with confining and controlling these energy-producing reactions. Initial active control approaches consisted primarily of a small number of SISO PID controllers. More recently, as the number of plasma parameters to be controlled has increased, more sophisticated controllers have been designed, implemented, and tested on a number of experimental fusion devices. Up to now, magnetic fusion research devices have not been capable of hosting a plasma with the number and frequency of fusion reactions sufficient to produce more output power than is consumed in confining and controlling the plasma. This is about to change with anticipated completion of the ITER tokamak currently under construction in southern France [1]. Early operation of ITER will focus on learning how to produce and control plasmas that are far more energetic than in any existing magnetic-confinement device. The initial plasma control system is being designed now, including both the software architecture and the algorithms that will be used for control during ITER first plasma operation starting in approximately 2025.

*This material is based upon work supported by the U.S. Department of Energy, Office of Science, Office of Fusion Energy Sciences, using the DIII-D National Fusion Facility, a DOE Office of Science user facility, under Awards DE-FC02-04ER54698, DE-SC0010661, and DE-SC0010537.;Disclaimer:This report was prepared as an account of work sponsored by an agency of the United States Government. Neither the United States Government nor any agency thereof, nor any of their employees, makes any warranty, express or implied, or assumes any legal liability or responsibility for the accuracy, completeness, or usefulness of any information, apparatus, product, or process disclosed, or represents that its use would not infringe privately owned rights. Reference herein to any specific commercial product, process, or service by trade name, trademark, manufacturer, or otherwise does not necessarily constitute or imply its endorsement, recommendation, or favoring by the United States Government or any agency thereof. The views and opinions of authors expressed herein do not necessarily state or reflect those of the United States Government or any agency thereof.; ITER is a Nuclear Facility INB-174. The views and opinions expressed herein do not necessarily reflect those of the ITER Organization.; This work is supported in part by the Swiss National Science Foundation.

M. L. Walker (walker@fusion.gat.com) is with General Atomics, San Diego, CA 92121, USA.

P. De Vries (Peter.DeVries@iter.org) is with ITER Organization, St Paul Lez Durance, France.

F. Felici (federico.felici@epfl.ch) is with EPFL - Swiss Plasma Center, Lausanne, Switzerland.

E. Schuster (schuster@lehigh.edu) is with the Department of Mechanical Engineering and Mechanics, Lehigh University, Bethlehem, PA 18015, USA.

II. MAGNETIC-CONFINEMENT FUSION

A. Objectives of Fusion

The fusion process[1] proposed for power generation combines two hydrogen isotopes - deuterium (D) and tritium (T) - to produce a helium nucleus (also known as an α particle), a neutron, and thermal energy. In this fusion reaction (and any nuclear reaction, including fission), a small amount of mass is converted into energy. Twenty percent of this energy is thermal - associated with the charged products that remain in the plasma - and goes to support the continued reaction. The remaining 80% is in the free neutron that is captured by the walls of the fusion reactor and its energy is converted to heat. The heat from captured neutrons can be subsequently converted to electrical energy. The fraction of mass "lost" is tiny, just 38 parts out of 10,000. Nevertheless, fusion energy released from just 1 gram of deuterium-tritium fuel equals the energy from about 2400 gallons (7.4 tons) of oil.

For the two isotopes to fuse together the nuclei must collide, but their similar positive electric charges creates a repellent force between them. This force can be overcome by causing them to collide at sufficiently high speed. These high-speed interactions can be produced by heating the gases to sufficiently high temperatures; increasing the gas density increases the frequency of particle collisions. Creating the conditions for frequent high-speed collisions is a primary objective of controlled nuclear fusion.

Assuming that such collisions can be produced in a controllable manner, a fusion power plant would use a concept similar to a power plant that burns coal or oil. A heat source boils water and produces high-pressure steam, which turns a turbine generator to produce electricity. A power-producing fusion reactor would simply use a different heat

[1]This paper expands on concepts and results previously described in [2],[3],[4]]. Some repetition of these concepts is required in the initial sections to make this work self-contained.

source (fusion). A significant difference from conventional is that fusion requires millions of times less fuel for the same amount of steam and electricity. In fact, there is sufficient fuel for thousands of years. Deuterium can be extracted from the inexhaustible supply in sea water (1 part/ 6,500 parts H_2O). Tritium can be produced from lithium inside the reactor itself, where lithium extracted from ocean water is enough for millions of years [5].

Fusion energy has other advantages. It does not produce any of the compounds responsible for global warming. (In fact, there is currently a global shortage of its primary reaction product, helium.) There is virtually no risk of nuclear accident, since (in contrast to fission) meltdown is not possible because an uncontrolled energy increase leads to self-shutdown of the reaction. A fusion power plant would produce no high level radioactive waste (e.g., no fission fragments) - only a small volume of activated reactor components with short lived radioactivity (10 years vs 10 thousand years for fission).

However, constructing an energy-generating fusion reactor is challenging, since not only must the deuterium and tritium nuclei be heated to very high temperatures, but the hot gases must also be confined in a small enough volume for a statistically large number of D-T collisions to occur. This is where magnetic confinement comes in.

B. Tokamaks

The magnetic confinement approach to constructing a fusion reactor is to ionize neutral hydrogen gas isotopes, resulting in a plasma. This plasma, consisting of electrically charged particles, can be held within a fixed volume through use of magnetic fields created by large electrical currents. The plasma is then heated to sufficiently high temperatures to induce fusion reactions.

There are several variations of magnetic confinement, but the concept that is the most mature uses a toroidal device called a tokamak. All tokamaks use the same basic concept, illustrated Fig. 1. All tokamaks produce plasma *pulses* (also referred to as *shots* or *discharges*) comprising approximately the same sequence of events. These events can be illustrated using the DIII-D experiment [6] as a typical example (Fig. 2). Time during the discharge is measured relative to t=0, the approximate time at which plasma is initiated. Current in the toroidal field (TF) coil (brown in Fig. 1) - known as the B-coil at DIII-D - is brought up early to create a constant toroidal magnetic field to confine the plasma when it is initially created. Just prior to t=0, deuterium gas is puffed into the interior of the torus-shaped containment vessel (gray in Fig. 1), and the ohmic heating coil (magenta in Fig. 1) - known as the E-coil at DIII-D - is brought to its maximum positive current in preparation for plasma initiation.

At $t = 0$, the E-coil current is driven down quickly to produce a large electric field within the torus. This electric field accelerates free electrons, which collide with and rip apart neutral gas atoms, thereby producing ionized gas or plasma (red torus in Fig. 1). The plasma consists of charged particles that are free to move, and thus acts as a conductor.

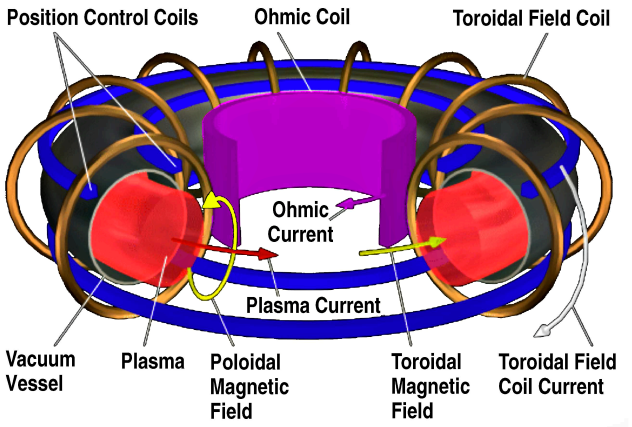

Fig. 1. Illustration of magnetic confinement in a tokamak.

Consequently, immediately after plasma initiation, the ohmic coil current, which is commanded to continue its downward ramp, now operates as the primary side of a transformer whose secondary is the conductive plasma. This transformer action causes current to flow in the plasma by means of the opposing flows of oppositely charged particles. This effect is known as *inductive current drive*. Collisions of the electrons and ions cause the plasma to be resistive, which causes the plasma to heat (thus the origin of the term *ohmic heating*). The rate of ohmic coil current decrease is used to control the plasma current I_p up to a target *flat-top* level by about 1 second after plasma initiation. At the same time, currents driven in poloidal field (PF) coils (blue in Fig. 1) confine and shape the plasma, to prevent it from contacting the vessel wall and to produce desirable fusion performance characteristics. The combination of toroidal field B_ϕ produced by TF coil currents and poloidal field B_p (orthogonal to B_ϕ) produced by PF coil and plasma currents results in a helical magnetic field around the torus (Fig. 3).

Shortly after $t = 0$, additional gas is puffed into the chamber to increase density and pressure to desired levels. In most DIII-D discharges, neutral beams (uncharged atoms of deuterium) are injected into the plasma at high velocity. These particles collide with particles in the plasma, thereby converting their momentum into heat and further heating the bulk plasma. When directed toroidally into the plasma, this momentum can also be used to provide torque for plasma rotation and to drive plasma current. Various forms of radio-frequency (RF) actuators (with action similar to your microwave oven) are also employed to heat and drive current in plasma. One system (the electron-cyclotron (EC) heating and current drive system - (ECRH/ECCD) can preferentially control the location and direction of heating power and driven current by use of steerable beam-injection mirrors. NBI and RF actuators both generate what is known as *non-inductive current*. Another source of non-inductive current is the so-called *bootstrap current*, which is self-generated by the plasma when a density gradient is present [4].

The separate time intervals in which the plasma current is increasing (0 to 1 second), constant (1 to 5 seconds),

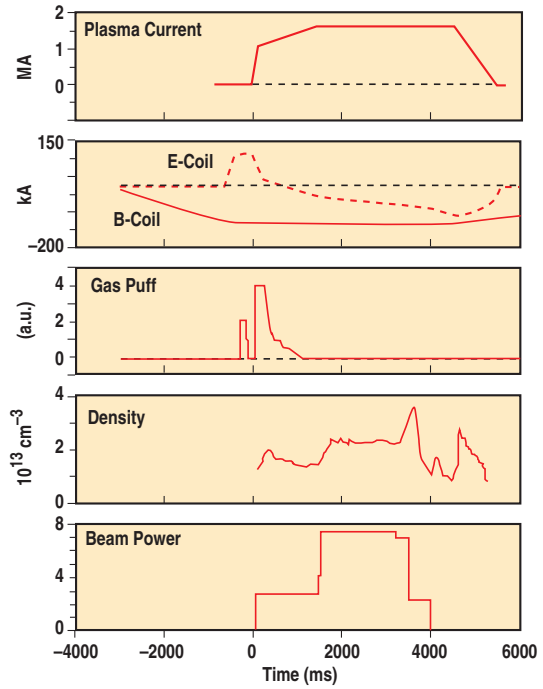

Fig. 2. Evolution of a plasma in the DIII-D tokamak

or decreasing (5 to 6 seconds) are often referred to as, respectively, the *rampup*, *flattop*, and *rampdown* phases.

There are currently several experimental tokamaks around the world [2]. Every tokamak is different, with capabilities designed to support a particular experimental goal. Each is designed to operate with a different maximum plasma current level (a few hundred kilo-Amps to a few Mega-Amps), toroidal field (a few Tesla), and duration of discharges. Nearly all use some form of active plasma control, with several actively conducting research to address existing and future plasma control needs.

Although Fig. 1 illustrates a plasma with a circular cross-section, obtaining high performance generally dictates a non-circular cross-section [7]. Fig. 4 illustrates the cross-section of an experimental plasma in the DIII-D tokamak, represented by a set of contours representing points of constant poloidal flux Ψ. To understand this figure, it is necessary to understand the notion of flux coordinates. The standard definition of magnetic flux is the integral of magnetic field normal to a specified surface $\Psi = \int_S B \cdot dS$. For fusion plasmas, this definition is extended to define flux at a point $P = (R,Z)$ in a poloidal cross-section as the flux through an imaginary disk (Fig. 3) whose boundary passes through (R,Z). Contours in Fig. 4 represent curves of constant flux according to this extended definition.

Flux has largest absolute value at the center of these nested flux contours at the *magnetic axis*. The closed flux contour farthest from the magnetic axis (also called *last closed flux surface* or *separatrix*) defines the edge of the plasma. In a *diverted plasma*, the separatrix forms an *X point*, in Fig. 4 at the bottom of the plasma. (It is also possible to have a *limited plasma*, in which the separatrix is defined as the contour tangent to or "touching" the vessel wall.) The points at which

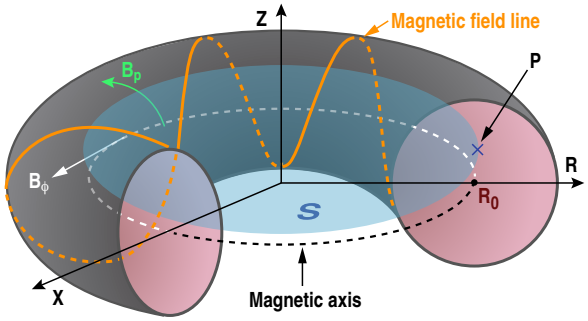

Fig. 3. Illustration of (helical) total field B equal to the sum $B = B_p + B_\phi$ of poloidal and toroidal field vectors, and of flux Ψ at a point $P = (R,Z)$.

a diverted plasma separatrix strikes the vessel wall are *strike points*. The location of the separatrix and the X point (or strike points) are controlled (as discussed in Section IV) by the poloidal field generated by currents in the PF coils (whose cross sections are labeled F1A through F9B here).

The nesting of contours of constant flux Ψ in Fig. 4 is predicted by ideal MHD theory and confirmed by experimental measurement. The complete representation shown cannot be measured directly, so is produced by an algorithm that fits an ideal MHD model known as the Grad-Shafranov (GS) equation to measurements from magnetic sensors attached to the vessel wall or just outside of it. The GS equation is given by

$$-\Delta^* \psi = \mu_0 R^2 \frac{\partial p}{\partial \psi} + f \frac{\partial f}{\partial \psi}, \tag{1}$$

where p and f are fitted-parameter functions [8], μ_0 is vacuum magnetic permeability, $\psi = \Psi/(2\pi)$, and the Δ^* operator is

$$\Delta^* \psi = R \frac{\partial}{\partial R}\left(\frac{1}{R}\frac{\partial \psi}{R}\right) + \frac{\partial^2 \psi}{\partial z^2}. \tag{2}$$

There are several types of magnetic sensors, distinguished by whether they measure local magnetic field, magnetic flux through a surface, current in coils driven by power supplies, or current induced in conducting structures or plasma. For most tokamaks, there are a few hundred such measurements. Other sensors make additional measurements that can also be used to constrain the fit by characterizing internal parameters such as temperature, pressure, or internal magnetic field. As with magnetic sensors, these internal-parameter sensors must by necessity be remote from the plasma because of high temperatures, radiation effects, or both.

When applied external magnetic field forces (magnetic pressure) balance kinetic pressure within the plasma so that the plasma does not move or deform (Fig. 4), the plasma is in equilibrium. This equilibrium constitutes part of the overall operating point of the controlled system.

III. TOKAMAK CONTROL NEEDS

Control needs for tokamaks are driven largely by the long-term goal of putting energy on the grid. Economic factors dictate the need for high-fusion-performance plasmas, which are invariably either unstable or marginally stable. Efforts

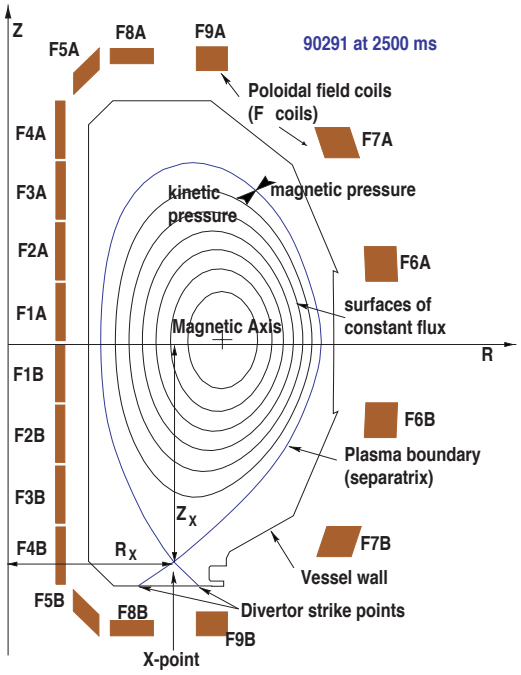

Fig. 4. Cross section of the DIII-D tokamak showing a flux contour representation of the plasma.

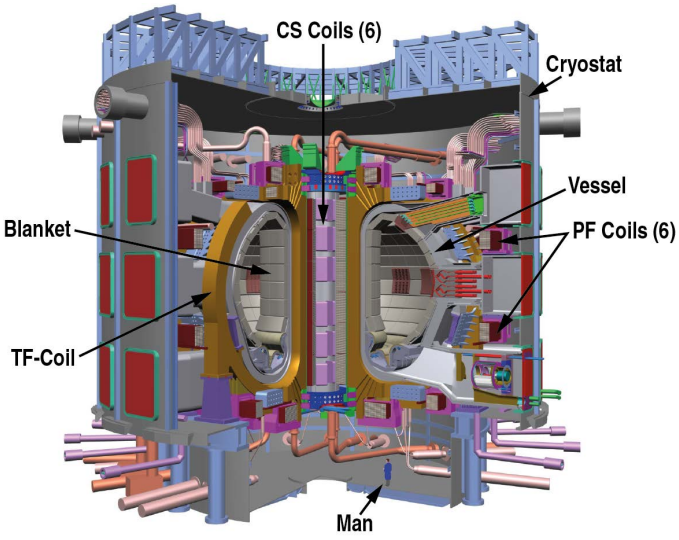

Fig. 5. The ITER tokamak. The cryostat is a large tank filled with supercritical helium to cool the superconducting coils. Blanket modules protect the vessel walls from the intense heat of the plasma. The central solenoid (CS) coils are PF coils whose purpose includes acting as a virtual ohmic coil. Note man for scale.

to reduce plasma instability while maintaining or increasing performance lead to two separate but interdependent approaches - active stabilization by feedback control and search for system operating points with improved passive stability. Research into operating point modification is generally conducted by plasma physicists, since it requires deep understanding of plasma physics. However, it also requires active control to gain access to and regulate around a chosen operating point. At the same time, minimization of plant cost (economics again) leads to small control margins, with a concomitant increased potential for loss of control. This non-negligible risk implies the need for robust mechanisms to detect or predict incipient loss of control and respond in a way that minimizes negative impact of that loss of control.

The previously-mentioned ITER tokamak (Fig. 5) is the near-term target of a significant part of ongoing plasma control research since its operation will depend critically on control. ITER already has several of the characteristics of envisioned fusion power reactors. Most importantly, it will be the first device to demonstrate a self-sustained fusion reaction (referred to as burn). It will also operate pulses with long duration characteristic of a real reactor. ITER plasmas are projected to generate approximately 10 times more output fusion power than input power (*fusion gain* $Q \geq 10$) when fully operational. However, ITER is not actually electricity-producing and will not connect its output power to the electrical grid. Instead, it will be used to understand scientific and technical issues related to sustainment of a burning plasma and, ultimately, to demonstrate feasibility of fusion as an energy source. ITER is huge (see man at bottom right of Fig. 5 for scale) and expensive (billions of dollars), so is being built by a multi-country consortium that includes the EU, Japan, USA, China, India, South Korea, and Russia.

Energy-producing fusion power plants (and even ITER) require control performance and robustness comparable to high performance aircraft (e.g., jet fighters). Similar to high performance aircraft, fusion plasmas are intrinsically unstable (although closed loop stable), operate near the edge of technologies' performance envelope, and yet must operate with high robustness to disturbances and even system faults. However, in contrast to aircraft, the tokamak and plasma are completely under autonomous control by a real-time Plasma Control System (PCS). Controlling automatically all aspects of a tokamak discharge is a challenging task. Actuator and sensor capabilities are limited and can compromise control performance when operating the tokamak at its highest performance. The control must also avoid a number of operational limits related to stability of the plasma itself. Uncontrolled growth of instabilities can lead to deterioration of the plasma confinement, yielding a disruptive end of the discharge [9]. During such a discharge *disruption* the thermal and magnetic energy is dissipated onto the device in a very short time (ms to hundreds of ms in ITER), yielding very high thermal and electro-magnetic loads. Such events should to be prevented and, if this is not possible, mitigating action must be taken [10].

Energy content of plasmas produced during the "first plasma" phase of operation are very small when compared with plasmas planned for later operation phases, which means that consequences of most possible control failures are similarly small. However, even during "first plasma" operation there are certain control failures that can lead to many millions of dollars of device damage. During later phases of ITER operation, the consequences of control failure will become more severe at the same time that requirements for control grow more complex. Thus low disruptivity operation is key to maintaining the integrity of the tokamak and is fundamentally a plasma control problem.

The PCS must actively regulate the plasma state to remain as (passively) stable as possible. Any instabilities that remain must be actively controlled and stabilized. In addition to continuously-acting control, the PCS must be able to detect and respond asynchronously to hardware faults and "off-normal" plasma conditions [11].

In the following we provide a more detailed discussion of three categories of plasma control. Axisymmetric control is discussed in Section IV, magnetic instability control in Section V, control of internal plasma quantities, including fusion burn, is discussed in Section VI. Finally, Section VII describes the emerging field of off-normal event handling.

IV. AXISYMMETRIC MAGNETIC CONTROL

Axisymmetric magnetic control refers to control of the plasma position and shape in the 2D poloidal plane, and of plasma current. Since the first tokamaks in the 1960s and 1970s, this type of control has been extensively studied, since it is necessary to keep the plasma in the desired position in the reactor vessel. Additionally it was soon found essential to avoid significant contact with the (cold) reactor walls in order to reach the high temperatures desired for fusion. This is to keep the plasma pure, mostly containing light nuclei (Deuterium and Tritium), and avoiding contamination with heavier elements that may be present in the material of the wall. This field of research is relatively mature, and several tutorial papers and books have been published, e.g. [3], [12]. Here, we present a brief tutorial introduction to the problem and refer to references for more detail.

A. Plasma current and position control

As explained in the introduction, a plasma equilibrium features a toroidal electrical current (I_p) in the conducting plasma. Since many properties of the plasma (stability, confinement) are strongly affected by the value of the plasma current, it is typically regulated. It is ramped from zero (at the beginning of the discharge), maintained at a desired set-point value for the duration of the plasma, then ramped back down to a low value before the plasma is extinguished. Additionally, the position of the plasma in the (R,Z) plane must be controlled to avoid wall contact. Together, the control of (R,Z,I_p) requires a basic set of 3 feedback loops that any tokamak must have in order to function effectively.

1) Plasma current control: In most cases, the plasma current is driven by induction (Section II-B). The so-called central solenoid (Fig. 5), a set of magnetic coils close to the vertical axis of the device, is used for this purpose, as it is designed to change the poloidal magnetic flux (which drives current inductively), while having a low magnetic field in the plasma region (which would affect the plasma position - see Radial Position Control, below). A simplified equation for the dynamics of the plasma current, in case of a single solenoid coil, can be written as:

$$0 = M_{pc}\dot{I}_c + L_p\dot{I}_p + R_pI_p, \tag{3}$$

Where M_{pc} is the mutual inductance between the plasma current distribution and central solenoid coil, L_p is the plasma self-inductance and R_p is the plasma resistance. I_c, I_p are the coil and plasma currents, respectively.

This equation is coupled to the circuit equation for current in the coil

$$L_c\dot{I}_c + R_cI_c + M_{cp}\dot{I}_p = V_c \tag{4}$$

Where L_c is the coil self-inductance, R_c is the coil resistivity, and $M_{pc} = M_{cp}$ as previously defined.

From equation (3) one can observe that a constant $I_p > 0$ requires a time-varying I_c, i.e., $\dot{I}_c < 0$. Indeed, the SISO transfer function from V_c to I_p is written as:

$$\frac{I_p(s)}{V_c(s)} = \frac{M_{pc}s}{M_{pc}^2s^2 - (L_cs+R_c)(L_ps+R_p)} \tag{5}$$

Since this transfer function features a zero at the origin, it requires at least two integrators in the controller to control the plasma current with zero steady-state error.

2) Radial position control: Since the plasma carries an electrical current, magnetic fields (self-generated or applied externally through magnetic coils) result in a Lorentz force on the plasma, following the equation $\mathbf{f_L} = \mathbf{j}\times\mathbf{B}$, where $\mathbf{f}_L$ is the force density, $\mathbf{j}$ the plasma current density, $\mathbf{B}$ the magnetic field vector. This force has to balance the pressure gradient in the plasma everywhere in space, a condition known as the MHD force balance.

The main effect of the plasma pressure is to push the plasma radially outward, in a similar fashion as the outward force on a pressurized tire. Another outward force, known as 'hoop force', occurs due to compression of the magnetic field on the inside part of the torus. To counteract this force, a vertical magnetic field is applied by a set of 'vertical field coils', which, in combination with the toroidal plasma current, generates an inward radial force that compensates the plasmas outward radial force (see left half of Fig. 6). Since the required radial force will vary depending on the plasma pressure, another feedback loop known as radial position control is used to keep the plasma at the desired radial location. A simple model for the dynamics of the radial position can be written as:

$$m_p\frac{d^2R}{dt^2} = \frac{\mu_0 I_p^2}{2}\Gamma(R,\beta_p,l_i) + 2\pi RI_pB_Z(R,Z,I_r,I_v), \tag{6}$$

Where m_p is the plasma mass, R is the plasma radial position (Fig. 3), Γ is a factor that depends on internal quantities of the plasma (mainly the normalized pressure $\beta_p = \frac{<p>}{B_p^2/(2\mu_0)}$, where $<>$ indicates an average over the plasma volume, and the normalized internal inductance per unit length $\ell_i = (\frac{L_i}{2\pi R_0})/(\frac{\mu_0}{4\pi})$, where $L_i = 2\int_P \frac{B_p^2}{2\mu_0}d\mathbf{r}/I_p^2$ and P is the plasma volume), and B_z is vertical field generating the counteracting inward Lorenz force [8]. Since the plasma mass is very small, one can consider the limit $m_p = 0$ and assume the plasma instantaneously satisfies this force balance equation, with the position determined by the (slower) time-evolution of the two forcing terms on the right-hand-side. B_z depends on the spatial position of the plasma, as well as on the current in the radial position control coils I_r and any other currents in the surrounding vessel structure (I_v).

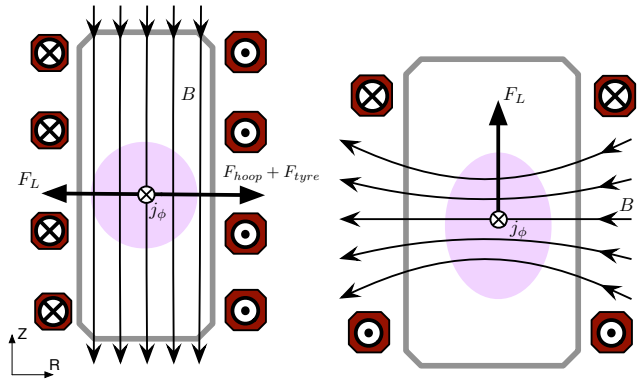

Fig. 6. Illustration of vertical field used to balance the radial outward forces of a tokamak plasma (left), and radial field used to stabilize the vertical position (right). Typical coil current arrangements to generate such fields are shown as well, with top and bottom coils at the same radius on the right connected in anti-series. Crosses indicate currents pointing into the page, and points indicate currents pointing out of the page.

$$I_p\frac{\partial B_R}{\partial z}=0,\kappa=1,n=0 \qquad I_p\frac{\partial B_R}{\partial z}<0,\kappa>1,n<0$$

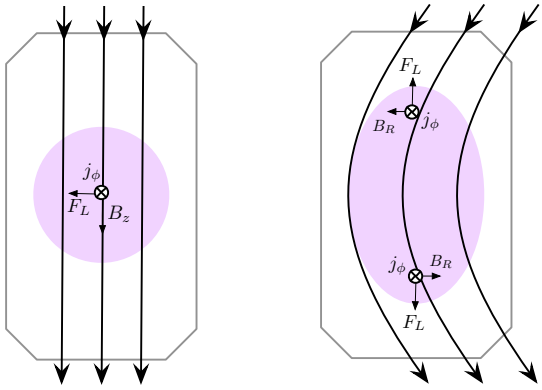

Fig. 7. A purely vertical magnetic field yields a circular plasma ($\kappa=1$). Adding curvature to the magnetic field results in elongated plasma ($\kappa>1$), which is vertically unstable. F_L indicates the Lorentz force produced by current density j_ϕ (into the page) and magnetic field B

Since the current in the coils is, in steady state, proportional to the applied voltage, a PID controller is sufficient to control the radial position to a desired set-point value.

3) Vertical position control: The third control loop is the so-called vertical stability loop. This is the most complicated position control loop since the open-loop plant is inherently unstable in the vertical direction. For reasons related to detailed physics of magnetic confinement, plasmas with a vertically elongated shape (such as in Figure 4) have higher pressure than circular plasmas. To obtain an elongated plasma, a curved field must be applied (Figure 7, right). Intuitively, one can think that this curved field has the effect of applying an upward force on the top half of the plasma, and a downward force on the lower half of the plasma, resulting in an elongating effect. Unfortunately, this same field makes the plasma position vertically unstable: a small vertical displacement will increase the vertical force in the direction of the displacement, leading to an instability. This instability is partially counteracted by the eddy currents (currents induced in surrounding conducting structures due to the moving plasma current column). The growth rate of resulting instability can be rather fast, with a real pole up to 1000s^{-1} for some tokamaks. The instability can be stabilized by acting on a combination of coils that generate a radial magnetic field (as illustrated in right half of Fig. 6), which induces a vertical force on the plasma. In many tokamaks with high elongation (hence having high growth rates of the vertical instability), specialized 'fast coils' are placed close to the plasma to react more rapidly to the plasma displacement.

Since there are no net forces on a plasma equilibrium in the vertical direction, a linearized model of the vertical position dynamics around an equilibrium can be used [12]. This model must include the coupling to the 'eddy currents' induced in the vacuum vessel as a reaction to changing magnetic fluxes.

$$\begin{aligned}\delta z-\frac{2R_0}{\mu_0 I_{p0}\Gamma n}\frac{\partial M_{pv}}{\partial Z}\delta I_v-\frac{2R_0}{\mu_0 I_{p0}\Gamma n}\frac{\partial M_{pz}}{\partial Z}\delta I_z&=0\\ M_{vv}\dot{I}_v+R_vI_v+I_{p0}\frac{\partial M_{vp}}{\partial Z}\delta\dot{z}+M_{vz}\dot{I}_z&=0\\ L_z\dot{I}_z+R_zI_z+I_{p0}\frac{\partial M_{vp}}{\partial Z}\delta\dot{z}+M_{zv}\dot{I}_v&=V_z\end{aligned}\tag{7}$$

Here δ indicates the variation of a quantity with respect to its equilibrium value, n is the curvature index defined as $n=-\frac{R_0}{B_{z0}}\frac{\partial B_R}{\partial z}$, (with B_{z0} the vertical magnetic field generated by the coils at the plasma position, and R_0 the radial coordinate of the center of the vacuum region). I_z is the current in the anti-series coil combination used for vertical position control, and I_v is a (vector) of vessel currents in the surrounding structure. Substituting δz from the first equation into the last two, a model is obtained with two real poles, of which one is unstable, and an unstable zero. This system can be stabilized by a PD controller but, as is well-known from classical control theory, an unstable system with a zero imposes limitations on the control performance. Additionally, the presence of delays will lead to further reduction of the maximum attainable control performance. [13].

In practice, the (R,Z,I_p) control loops are often analyzed simultaneously by combining the equations of all the coils, the radial force balance, the vertical force balance and the plasma current, as well as measurement equations for all the magnetic field, flux and current measurements.

The resulting model, which represents the dynamics of the tokamak modeling the plasma as a rigidly displacing conductor, is referred to as the Rigid Plasma Displacement Model. Despite its simplicity, it covers the most important dynamics required for a design of a position and current controller. The simplifications in the modeling result in controller gains that are not directly applicable to the real tokamak. For this reason, PID-type controllers are usually designed so that gains of each loop have effects that can easily be interpreted, so that they can be manually tuned as required based on experimental findings. Alternatively, more accurate models can be used to directly synthesize controllers, as discussed in the next section.

4) Plasma shape control: As mentioned before, the shape of the plasma in the 2D poloidal plane has a significant

effect on the plasma performance. By shape we mean the location of the Last Closed Flux Surface (LCFS) as well as the configuration of the divertor region (see discussion for Fig. 4). Since the flux distribution, and hence the location of the LCFS, depends on the magnetic fields, the shape of the externally applied magnetic fields affect the shape of the plasma and of the divertor region.

A first step for controlling the shape is to be able to directly control the current of any remaining magnetic coil combinations (after having used three coil combinations for the three control loops for R,Z, and I_p). This is usually done with another set of PID control loops for each circuit. Then, the plasma shape can be controlled using pre-calculated feedforward references for these coil currents. Indeed, the coil currents required to obtain a desired plasma shape can be quite accurately determined by solving the MHD force balance, coupled to time-varying equations for the coil and vessel currents. Ad-hoc corrections to these coil currents are often employed in a shot-to-shot, trial-and-error (and time-consuming) fashion to compensate for unmodeled disturbances. To avoid these manual corrections, many existing tokamaks employ feedback control to change the coil current references in order to control plasma shape. This shape control loop is often an additional, external loop closed after the (R,Z,Ip) and coil current control loops have been closed, though other approaches also exist. This hierarchy of controllers is schematically shown in Fig. 8.

Two main approaches exist for shape control: control of Gaps or Isoflux control. In the first approach, the distance between the plasma LCFS and the first wall is controlled to a desired value. In the second approach, the differences between poloidal flux values at various control points on the boundary are controlled to zero. To determine the control errors in real-time, one can either extrapolate magnetic measurements close to the plasma (which may not work well in the divertor region where the magnetic fields are low) or perform a real-time equilibrium reconstruction (solving the GS equation (1) in real-time, using constraints from measurements to determine the internal current distribution).

To obtain a model for designing a shape controller, the simplest approach is to neglect the plasma dynamics entirely and use the static relation between the currents in the coils and the fields to determine the expected change in plasma shape to changing currents. A more accurate (dynamical) model can be obtained by linearizing (1) around an equilibrium (e.g. [14]). Since the number of poloidal field coils may be different (sometimes smaller) than the number of shape errors, a non-square model of the plant is obtained. One then takes an SVD of the static gain of the plant to determine the error directions which can most easily be controlled [15], [16], [17], and design a diagonal PID controlling the errors projected on the principal singular vectors. Still, there often is an important component of feedforward control action, either computed in real-time or off-line to determine the currents required to obtain a desired shape.

To make these controllers of practical use, they must also take into account input constraints (saturation of power

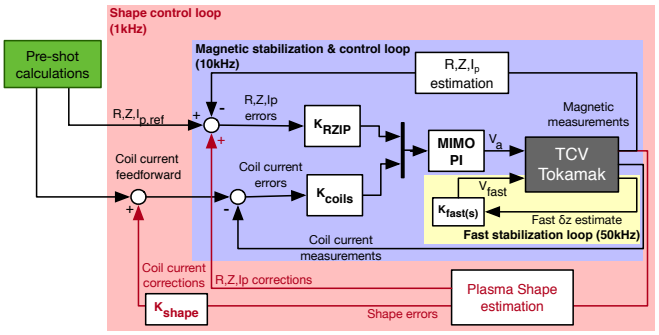

Fig. 8. Schematic diagram illustrating magnetic control as implemented in the TCV tokamak [16]. Note that three control loops are used, each running at different frequencies. A fast loop (yellow) controls the fast internal coil for vertical position stabilization. A slower set of loops (blue) control the plasma current, plasma position, and coil currents. The slowest, outer loop (red) controls the plasma shape and other quantities. Similar hierarchical control loops are used on various tokamaks.

supply voltages), input delays (due to digital control or power supply dynamics), state constraints, including nonlinear ones (maximum current, maximum heat dissipated in coils, forces between coils). To treat these operational limits, more advanced approaches such as MPC [18] have been proposed. Also, there is a wide literature on use of model-based modern multivariable control techniques on the tokamak control problem, including H-infinity control [19], [20], Kalman filtering for plasma state estimation [21], and more. However, perhaps surprisingly, these solutions are not routinely used for operating real-life tokamaks, to date, where individual PID controllers (with some decoupling scheme) are the norm [15], [22], [23], [16], [24]. One principal reason cited by tokamak operators is the lack of interpretability of results. When the controller does not perform as expected, one needs detailed knowledge of control theory/control mathematics to resolve the problem. Here, it is important to realize that the reality of tokamak operations is that control is a tool required to achieve plasma discharges that are then studied (for physics reasons, e.g. physics model validation, investigation of a physical effect, etc.). Any perceived delay in tokamak operations due to introduction of more sophisticated, and not easily interpretable controllers, often results in reverting to more primitive (e.g. PID) controllers that are easier to tune, even if they take some trial-and-error attempts to obtain the desired result. At the same time, automated methods to tune the control gains for individual loops have proven very useful in practice [25], [23]. For next-generation tokamaks such as ITER, and future fusion reactors, controller design relying more accurately on models will become more important owing to the vastly higher cost of individual discharges, but this may not completely supplant the need for some degree of manual tuning. This will require a new generation of engineers trained in both control theory and tokamak physics, to be able to support the use of advanced controllers.

Though position and shape control are relatively mature fields, further challenges remain: a recurring issue when designing individual control loops is the effective decoupling of the shape and position control loops. In the scheme shown in Figure 8, this is achieved by sending position reference

corrections from the shape controller to the inner position control loop, while ensuring that the shape control does not attempt to modify the position or current.

Another emerging challenge is to adapt, in real-time, the references for the plasma shape and position to respond to changes by supervisory control decisions (refer to exception handling, section VII).

V. 3D INSTABILITY CONTROL

In the previous section we discussed axisymmetric control, i.e., control of the plasma properties averaged toroidally and represented in the 2D poloidal (R,Z) plane. However, there are important 3D effects that affect time-evolution of a tokamak plasma and its confinement qualities, that must be taken into account and, in many cases, controlled. While a comprehensive review is outside the scope of this paper, we give a flavor of the issues here. For further reference, the reader is referred to [2] for a control-oriented overview and to [26] for a physics introduction.

A. Error field, RWM control

Due to small misalignments in the mechanical assembly of a tokamak, the confining magnetic fields may not be completely axisymmetric. The non-axisymmetric component of the field is known as the error field. The toroidal plasma will have a tendency to deform (in 3 dimensions) aligning itself with this non-symmetric magnetic field. When the plasma pressure increases, these deformations will tend to grow, in practice limiting the maximum pressure that can be achieved by the plasma. For this purpose, external non-axisymmetric magnetic coils are used to compensate for these imperfections and try to restore a perfectly axisymmetric field. Recently, extremum-seeking methods were used to optimize this field in real-time [27].

Even with a perfectly axisymmetric field, at high enough pressure the plasma can helically deform, due to an instability known as the Resistive Wall Mode (RWM) which leads to a loss of confinement followed by a disruption. This deformation can be detected by magnetic probes surrounding the plasma, and controlled by so-called non-axisymmetric coils surrounding the plasma. These coils significantly differ from the poloidal field coils discussed in the previous part, since they generate a field that is not axisymmetric but can have a 3D structure. Modern control methods have been used to control such instabilities, for example [28], [29], and these are expected to play a role in ITER.

B. Sawtooth and NTM control

Next to global responses of the plasma, described above, localized 3D deformations of the plasma magnetic structure have also been widely observed. Here we discuss only those most relevant for real-time control: those that must be controlled to maintain the plasma at good performance (high pressure) and that can be affected by actuators.

One is the so-called sawtooth instability, which manifests itself as a periodic collape of the pressure in the innermost part of the plasma, leading to a redistribution of current and energy from the inner to the outer regions of the confined plasma. This has the beneficial effect of removing unwanted impurities from the plasma, in particular the 'Helium ash' that is the product of fusion reactions. However, these sawtooth crashes generate a perturbation of the plasma magnetic fields, which may trigger other unwanted instabilities.

The amplitude and period of the sawtooth crashes can be controlled in several ways. Highly localized current drive (typically by ECCD) has an effect of stabilizing (leading to more infrequent and larger sawtooth crashes) or destabilizing sawteeth (leading to more frequent and smaller crashes), depending on the localization of the driven current. This method of control has been investigated in detail (e.g. [30]), where it was shown that applying said current drive has the expected physical effect. Feedback control approaches have also been demonstrated e.g. [31] where the steering mirror angles were controlled in feedback to achieve a desired sawtooth period. It has also been shown that, since the sawtooth instability can be described by a simplified nonlinear model generating a limit cycle, synchronization techniques can be applied. By periodically varying the power of the ECCD source, the sawtooth frequency can be made to lock to the frequency of the power perturbation [32]. This is of practical interest, since it is highly beneficial to be able to control the sawtooth period precisely in order to regulate the mixing between core and peripheral plasma region, as well as to preempt any negative effects that the sawtooth crash has on the global plasma stability.

Another important class of instability is the so-called Neoclassical Tearing Mode (NTM). This is a 3D helical deformation of the plasma around certain flux surfaces where the magnetic field closes on itself in a rational number of turns around the torus. A cross-section view of this deformation is illustrated in Fig. 9, where 'magnetic island' can be seen on the poloidal plane. Since the island X-points connect two flux surfaces that would otherwise be separated, an NTM leads to a local increase of thermal transport, and therefore to decrease of the local plasma pressure gradient. This local reduction of the pressure gradient causes a decrease of the local bootstrap current, which in turn causes a change in the magnetic field that increases the size of the island. Appearance of an NTM can be triggered by the previously mentioned sawtooth crashes, or they may appear spontaneously, with a higher chance of being triggered at higher pressure. NTMs are metastable, meaning that often they are linearly stable, but if a perturbation generates a large enough seed NTM, its growth rate may be positive. If an NTM's size can be reduced below a given threshold, the growth rate will become negative and the mode will self-stabilize. Without suppression, an NTM might grow to a size large enough to couple to one of the previously mentioned external modes, degrade the confinement and cause a disruption.

NTMs can be controlled by providing localized current drive, again with ECCD, on the island location (Fig. 9). This localized current compensates for the loss of bootstrap current. In present-day experiments, current drive is often

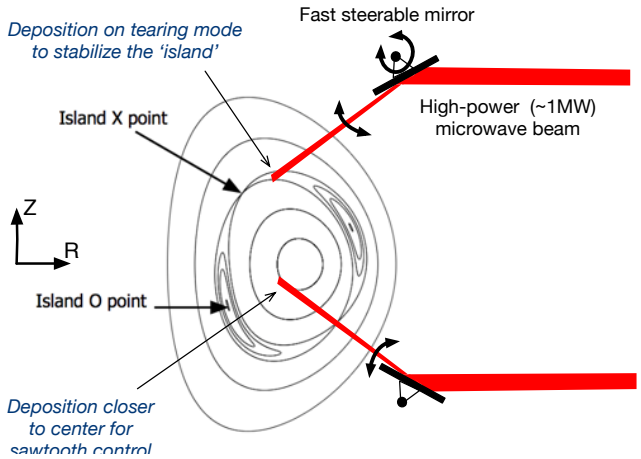

Fig. 9. Schematic illustration of simultaneous control of several MHD modes. An NTM is visible as a rotating 'island' in the poloidal plane. Driving current with EC actuators on the location of the mode can stabilize the island and restore the nested flux surface topology. Simultaneously, another EC actuator might be necessary to control the sawtooth instability, which occurs closer to the center of the plasma.

applied on the island location by trial-and-error feedforward positioning of the launcher steering mirrors. Significant research effort has been put into achieving this alignment using feedback control. Also here, automatic optimization algorithms based on extremum-seeking [33] as well as approaches requiring accurate calculations of the island location have been investigated [34]. Since accurate positioning of the microwave beam on the island is important, this places stringent requirements on the sensor accuracy for real-time estimation of the island position. Placing sensors in the same viewing line as the injected microwave beams may alleviate this problem [35].

One difficulty in MHD control for reactor-grade devices, is that the same (ECCD) actuators must be shared between different control tasks. They may be used for other control tasks when no NTM is present, while they must be repurposed to NTM control when NTMs appear. While many examples exist of dedicated experiments for NTM or sawtooth control, comparably few examples [36] exist of integrated control of multiple MHD instabilities. In a future tokamak, the choice of which MHD mode to control, with which actuator, must be made automatically. This is the subject of intense study in recent years [37], [38], [39], [40], [41], [42].

VI. CORE MAGNETIC AND KINETIC CONTROL

A fundamental control problem arising in tokamaks is the regulation of several properties of the core plasma such as density, temperature, current, and rotation since these properties are strongly linked to advanced modes of operation characterized by a high confinement state with enhanced magnetohydrodynamic (MHD) stability, which yields strong improvements in plasma performance. Such improvements are quantified by increases in energy confinement time, plasma pressure, and fusion power density (properties formally defined below). Moreover, in these advanced modes of operation a dominant fraction of the plasma current is self-generated by the neoclassical bootstrap mechanism [43],

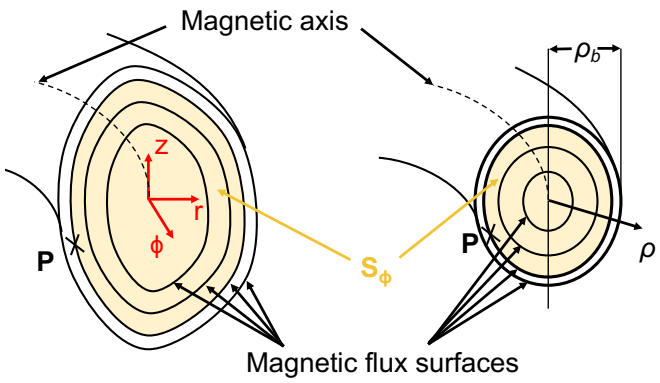

Fig. 10. Magnetic configuration in a tokamak.

which reduces the requirement on externally driven non-inductive current for steady-state operation. The dynamics of these core-plasma properties depend on both time and space. Their high dimensionality (infinite-dimensional PDE system), together with the nonlinearity exhibited by the dynamics of these properties and the limited actuation capabilities available in tokamaks, makes the regulation of both the magnitudes and the spatial profiles of these core-plasma properties one of the most challenging control problems in tokamaks.

A. Control of Plasma Profiles

Under ideal MHD conditions, the magnetic-flux surfaces in a tokamak (see discussion in (Section II-B)) form toroidally nested surfaces around the magnetic axis as shown in Fig. 10. The axisymmetry provided by the toroidal geometry, which is indeed an ideal assumption, together with the selection of a spatial coordinate indexing the nested magnetic-flux surfaces reduces the three-dimensional problem to just one dimension. The mean effective minor radius, ρ, which is related to the toroidal magnetic flux, Φ, and to the vacuum toroidal magnetic field at the geometric major radius R_0 (Fig. 3) of the tokamak, $B_{\phi,0}$, by means of $\pi B_{\phi,0}\rho^2 = \Phi$, can be used as the indexing variable. At any point P on a magnetic-flux surface, the toroidal magnetic flux subtended by that surface is defined as $\Phi = \int_{S_\phi} B_\phi dS_\phi$, where S_ϕ is the poloidal surface normal to the ϕ-axis depicted in Fig. 10. The mean effective minor radius is normalized as $\hat{\rho} = \rho/\rho_b$, where ρ_b is the value of ρ at the last closed magnetic-flux surface as depicted in Fig. 10. This non-dimensional variable $\hat{\rho}$ is the spatial coordinate generally used to model the spatial dependence of the plasma dynamics in tokamaks.

1) 1D Nonburning Plasma Dynamics: The pressure profile, p, is given by

$$p = n_e k T_e + n_i k T_i, \tag{8}$$

where n_e and n_i are the plasma electron and ion densities (units of # particles/volume), respectively, T_e and T_i are the electron and ion temperatures, respectively, and k is the Boltzmann's constant. The thermal energy, E, is given by $E = \frac{3}{2}p$ (units of energy/volume since kT_e and kT_i have units of energy, usually keV). Similarly to both the poloidal and

the toroidal magnetic fluxes, both the pressure p and thermal energy E are constant on a magnetic-flux surface.

a) Electron Density Dynamics: The electron density transport equation (EDTE) is approximately written as [44]

$$\frac{\partial n_e}{\partial t} = \frac{1}{\hat{H}\hat{\rho}}\frac{\partial}{\partial \hat{\rho}}\left(\hat{\rho}\hat{H}D_{n_e}\frac{\partial n_e}{\partial \hat{\rho}}\right) + S_e, \tag{9}$$

with boundary conditions $\partial n_e/\partial\hat{\rho}|_{\hat{\rho}=0} = 0$ and $n_e(1,t) = n_{e,bdry}(t)$, and where t is the time, D_{n_e} is the electron density diffusivity coefficient, and $S_e(\hat{\rho},t)$ represents any flux-surface averaged source or sink of electron density.

b) Electron Temperature Dynamics: When the heat diffusion is the dominant heat transport mechanism (transfer via convection or particle transport can also be modeled if necessary), the electron heat transport equation (EHTE) can be written as [44]

$$\frac{3}{2}\frac{\partial}{\partial t}[n_eT_e] = \frac{1}{\rho_b^2\hat{H}}\frac{1}{\hat{\rho}}\frac{\partial}{\partial\hat{\rho}}\left[\hat{\rho}\frac{\hat{G}\hat{H}^2}{\hat{F}}\left(\chi_e n_e\frac{\partial T_e}{\partial\hat{\rho}}\right)\right] + Q_e, \tag{10}$$

with boundary conditions $\partial T_e/\partial\hat{\rho}|_{\hat{\rho}=0} = 0$ and $T_e(1,t) = T_{e,bdry}(t)$, and where χ_e denotes the electron thermal conductivity and Q_e represents the electron heat sources.

c) Toroidal Rotation Dynamics: The dynamics of the toroidal angular velocity, ω_ϕ, which denotes the rate at which the plasma rotates toroidally in the tokamak, is given by the toroidal rotation equation (TRE) equation [44],

$$m_i\langle R^2\rangle\frac{\partial(n_i\omega_\phi)}{\partial t} = \frac{1}{\hat{\rho}\hat{H}}\frac{\partial}{\partial\hat{\rho}}\left(f_\phi\chi_\phi n_i\frac{\partial\omega_\phi}{\partial\hat{\rho}}\right) + t_\omega, \tag{11}$$

with boundary conditions $\partial\omega_\phi/\partial\hat{\rho}|_{\hat{\rho}=0} = 0$ and $\omega_\phi(1,t) = \omega_{\phi,bdry}(t)$, and where χ_ϕ is toroidal momentum diffusivity, m_i is the ion mass, and t_ω is the ion-torque deposition source.

d) Poloidal Magnetic Flux Dynamics: The dynamics of the poloidal stream function, ψ, which is related to the poloidal magnetic flux as $\Psi = 2\pi\psi$, is defined by the magnetic diffusion equation (MDE) [45],

$$\frac{\partial\psi}{\partial t} = \frac{\eta}{\mu_0\rho_b^2\hat{F}^2}\frac{1}{\hat{\rho}}\frac{\partial}{\partial\hat{\rho}}\left(\hat{\rho}D_\psi\frac{\partial\psi}{\partial\hat{\rho}}\right) + R_0\hat{H}\eta\, j_{ni}, \tag{12}$$

with boundary conditions $\partial\psi/\partial\hat{\rho}|_{\hat{\rho}=0} = 0$ and $\partial\psi/\partial\hat{\rho}|_{\hat{\rho}=1} = -(\mu_0R_0I_p)/(2\pi\hat{G}|_{\hat{\rho}=1}\hat{H}|_{\hat{\rho}=1})$, and where η is the space-dependent plasma resistivity, which is a nonlinear function of the electron temperature T_e, j_{ni} is the space-dependent non-inductive current sources, μ_0 is the vacuum magnetic permeability, and I_p is the plasma current. $\hat{F}$, $\hat{G}$, $\hat{H}$, D_ψ, f_ϕ, $\langle R^2\rangle$ are spatial profiles corresponding to a particular magnetic equilibrium. The safety factor, q, and the rotational transform, $\iota \triangleq 1/q$, which are measures of the pitch of the magnetic field lines, are defined as

$$\frac{1}{\iota(\hat{\rho},t)} \triangleq q(\hat{\rho},t) \triangleq \frac{d\Phi}{d\Psi} = -\frac{d\Phi}{2\pi d\psi} = -\frac{B_{\phi,0}\rho_b^2\hat{\rho}}{\partial\psi/\partial\hat{\rho}}. \tag{13}$$

Moreover, the toroidal current density, j_ϕ, is computed as

$$j_\phi(\hat{\rho},t) = -\frac{1}{\mu_0\rho_b^2R_0\hat{H}}\frac{1}{\hat{\rho}}\frac{\partial}{\partial\hat{\rho}}\left(\hat{\rho}\hat{G}\hat{H}\frac{\partial\psi}{\partial\hat{\rho}}\right). \tag{14}$$

Both the safety factor and the toroidal current density depend on the gradient of the poloidal stream function, $\theta \triangleq \partial\psi/\partial\hat{\rho}$. Therefore, it is common to speak interchangeably of the current profile, the q-profile, the ι-profile, the θ-profile, and the ψ-profile control. One of the main challenges associated with the control of core-plasma properties such as p, q and ω_ϕ is the development of control-oriented models [46], [47], [48] for the diffusive terms (D_{n_e}, χ_e, χ_ϕ, η) and the source terms (S_e, Q_e, t_ω, j_{ni}) that are accurate enough to correctly predict the plasma evolution for model-based control design purposes but simple enough to keep the control-design problem tractable.

2) Density, Temperature, and Pressure Profile Control: The control of density, temperature, and pressure profiles in tokamak plasmas is challenging because of limited actuation capabilities and a relatively poor understanding of particle transport phenomena. In principle, these profiles can be controlled by fueling mechanisms such as puffing of gas and injection of frozen-fuel pellets and by heating mechanisms such as neutral beam injection (NBI) and different sources of radio-frequency waves. It is believed that the gradient of the pressure profile around magnetic flux surfaces where q is a rational number can play a critical role in triggering certain types of MHD instabilities (see Section V). Moreover, certain density and temperature profiles are necessary to produce the self-induced non-inductive bootstrap current [43], which favors steady-state operation.

3) Current Profile Control: Shaping the current profile, usually defined in terms of the safety factor q or rotational transform ι profiles, has been demonstrated to be a key condition for realization of advanced plasma scenarios characterized by MHD stability, improved confinement, and possible steady-state operation (an operating scenario is roughly defined as a target operating point and the path used to reach that point). The achievement of some types of current profiles favors generation of a so-called "internal transport barrier" (a region where particle and heat transport are strongly reduced), which improves confinement and facilitates steady-state operation by enhancing bootstrap current. It has been demonstrated that current profile control can slow down, and possibly stop, temporal evolution of current profile peaking, which tends to develop due to the fact that the plasma temperature is higher in the core and plasma resistivity is inversely related to temperature. Reduction of this peaking effect also allows avoidance of some instabilities or disruptive events related to presence in the plasma of magnetic flux surfaces where q is a rational number, such as NTMs (see Section V-B).

As can be noted from (12), the dynamics of the poloidal magnetic flux can be modified through three different mechanisms: i- the plasma resistivity η (*diffusivity control*), which can be "actuated" by controlling the electron temperature profile by using different radio-frequency heating mechanisms such as ECH (electron cyclotron heating); ii- the non-inductive sources in j_{ni} (*interior control*) such as neutral beam injection (NBI) and radio-frequency current drives, which may include ECCD (electron cyclotron current drive),

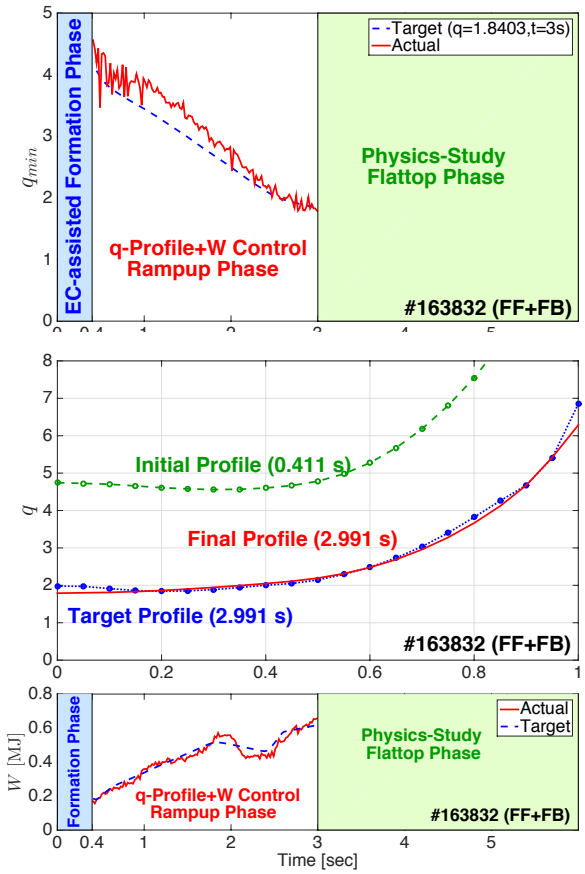

Fig. 11. Experimental test of feedforward + feedback q-profile controller based on off-line+on-line model-based optimization. Target q profile achieved at $t_f = 3{,}000$ ms while tracking a target W.

FWCD (fast wave current drive), LHCD (lower hybrid current drive), etc.; iii- the plasma current I_p (*boundary control*), which can be "actuated" by controlling the inductive component of the plasma current by transformer action.

Fig. 11 shows the performance of active control in DIII-D shot #163832. The goal was to drive both q and thermal stored energy W (defined as a volume-integrated quantity below), from a given initial state at $t_i = 400$ ms (end of plasma formation phase) to a target final state at $t_f = 3{,}000$ ms (start of physics-study flattop phase) by controlling individual on-axis and off-axis NBI powers, total EC power, and total plasma current. This target final state is characterized by a minimum value of q, denoted as q_{min}, of around 1.85, and a value of q at $\hat{\rho} = 0.95$, denoted as q_{95}, of around 5.5. A primary goal for the DIII-D research program is to develop the physics basis for a high q ($q_{\min} > 1.5 - 2.0$), high W, steady-state operation mode that can serve as the basis for future steady-state burning plasmas. The tight regulation of both q and W is made possible by combining off-line (feedforward control) [49], [50], [51] and on-line (feedback control) [52], [53], [54] model-based optimization (i.e., Model Predictive Control (MPC)). At the core of both optimizations are physics-based, control-oriented models of different complexities (off-line optimization: nonlinear model, on-line optimization: linearized model) capturing the dominant physics of q-profile and W responses to actuators.

4) Rotation Profile Control: Control of the toroidal rotation profile has recently attracted much attention because of its connection with MHD stabilization and advanced-mode access. As an alternative to active stabilization of RWMs by magnetic feedback control [28], [55], briefly discussed in Section V-A, experiments have shown that RWM passive stabilization is also possible by plasma toroidal rotation coupled with an energy dissipation mechanism. It has been shown that the critical rotation speed for RWM stabilization is a function of the rotation profile shape, implying a radially distributed stabilizing mechanism. RWM stability therefore depends on both β (a measure of plasma pressure, defined below) and toroidal angular velocity profile ω_ϕ. Unfortunately, RWM stabilizing rotation is often dissipated by drag torques generated by different mechanisms, including plasma fluid viscosity, and interaction between the plasma fluid with magnetic field perturbations. Modification of the rotation profile through active control [56], [57], in order to affect energy confinement, can improve stability of not only RWMs but also NTMs (see Section V-B). Other applications that might call for rotation profile control include: i- modification of the NTM rotation frequency to facilitate ECCD stabilization of the NTM as it rotates toroidally in the plasma, ii- establishment of conditions favorable for access to advanced operation modes (e.g., free of certain MHD instabilities). Neutral beam injection (NBI), and non-axisymetric magnetic field coils (the same coils that are used for RWM feedback stabilization) that allow modulation of the error fields (Section V-A) for magnetic braking (controlled drag torque), provide effective torque sources in (11) for control of the rotation profile in tokamaks.

B. Control of Plasma Scalars

Magnetic and kinetic profiles are very strongly and nonlinearly coupled in tokamak plasmas (note that the EHTE (10), TRE (11), and MDE (12) are coupled by means of both their diffusive terms (through η, χ_e, and χ_ϕ) and their source terms (through j_{ni}, Q_e, and t_ω)). Moreover, a single actuator may have strong effects on more than one plasma profile. It seems natural to try to develop an integrated magnetic and kinetic profile control algorithm. However, actuation resources are limited by design in tokamaks. Therefore, as we keep integrating control objectives, controllability issues arise. The question that follows is to what extent several control goals can be satisfied simultaneously. Due to actuation limitations, the "profile" control expectation for a given plasma variable may be reduced to its control at two or three locations at most. In some cases only control of a plasma variable at a single point or integrated over the plasma volume may be feasible. On the positive side, this may be enough for proper operation. This is particularly true when the control objective is given in terms of these volume-averaged plasma properties. For instance, thermal stored energy, W, is defined as

$$W(t) \triangleq \int_{V_p} E\, dV = \int_{\hat{\rho}=0}^{\hat{\rho}=1} E(\hat{\rho},t) \frac{\partial V(\hat{\rho},t)}{\partial \hat{\rho}} d\hat{\rho}, \qquad (15)$$

where V_p is the plasma region enclosed within the last magnetic-flux surface, and $V(\hat{\rho})$ is the plasma volume enclosed by the magnetic-flux surface labeled with $\hat{\rho}$.

1) 0D Burning Plasma Dynamics: By also computing volume-averaged values for densities of different species, it is possible, for instance, to model the dynamics of a DT plasma by using a zero-dimensional model:

$$\frac{dW}{dt} = -\frac{W}{\tau_W} + P_\alpha - P_{rad} + P_{Ohm} + P_{aux}, \tag{16}$$

$$\frac{dn_\alpha}{dt} = -\frac{n_\alpha}{\tau_\alpha} + S_\alpha, \tag{17}$$

$$\frac{dn_D}{dt} = -\frac{n_D}{\tau_D} + S_D^R - S_\alpha + S_D, \tag{18}$$

$$\frac{dn_T}{dt} = -\frac{n_T}{\tau_T} + S_T^R - S_\alpha + S_T, \tag{19}$$

$$\frac{dn_I}{dt} = -\frac{n_I}{\tau_I} + S_I + S_I^{sp}, \tag{20}$$

where n_D, n_T , n_α, and n_I are deuterium, tritium, alpha-particle and impurity densities, respectively, $P_\alpha \triangleq S_\alpha Q_\alpha$ is the alpha-particle heating from fusion reactions, $S_\alpha = n_D n_T \langle \sigma v \rangle_{DT}$ is the source of alpha particles (i.e., ${}^4_2He$ particles), $\langle \sigma v \rangle_{DT}$ is the DT reactivity, $Q_\alpha = 3.52$ MeV is the energy deposited in the plasma by each alpha particle, P_{rad} is the radiation losses, P_{Ohm} is the ohmic heating and P_{aux} is the controlled auxiliary power, S_D^R, S_T^R and S_I^{sp} are particle fluxes resulting from plasma-wall interactions, while S_D, S_T and S_I are the controlled injection rates of deuterium, tritium and impurities, respectively. Electron density is given by the quasi-neutrality condition (# electrons = # protons)

$$n_e = n_D + n_T + 2n_\alpha + Z_I n_I, \tag{21}$$

where Z_I is the impurity atomic number. The ion density is given by $n_i \triangleq n_D + n_T + n_\alpha + n_I$, whereas the total plasma density is simply $n = n_e + n_i$. The energy confinement time, τ_W, is modeled by scaling it with key plasma and machine parameters. The IPB98(y,2) scaling law is given by

$$\tau_W = 0.0562 H I_p^{0.93} R^{1.97} B_\phi^{0.15} M^{0.19} \varepsilon^{0.58} \kappa^{0.78} n_e^{0.41} P_{total}^{-0.69}, \tag{22}$$

where H is a constant that depends on the quality of the plasma confinement, R is the plasma major radius, M is the effective mass, $\varepsilon = a/R$ is the aspect ratio, a is the plasma minor radius, κ is the vertical elongation, $P_{total} = (P_\alpha - P_{rad} + P_{ohm} + P_{aux}) \times V$ is the total plasma power in MW, and V is the plasma volume. The ITER values of the parameters in (22) are listed in [58]. The particle confinement times are scaled with the energy confinement time τ_W such that $\tau_\alpha = k_\alpha \tau_W$, $\tau_D = k_D \tau_W$, $\tau_T = k_T \tau_W$ and $\tau_I = k_I \tau_W$, where k_α, k_D, k_T and k_I are constants.

The fusion power density for the DT reaction is given by

$$P_f = 5P_\alpha = n_D n_T \langle \sigma v \rangle_{DT} Q_{DT}, \tag{23}$$

where $Q_{DT} = 5Q_\alpha = 17.6$ MeV. The DT reactivity $\langle \sigma v \rangle$, which is the average of the cross section σ (probability of fusion) over a Maxwell-Boltzmann distribution of the velocity field, is a function of the plasma temperature as shown in Fig. 12. The DT reaction appears as the most promising not only because of its relatively large release of energy per reaction, Q_{DT}, but also because of the fact that the reactivity reaches the highest value at the lowest temperature when compared with other reactions. As can be noted from the figure, the reactivity increases as the temperature increases, which in turn produces more fusion power density and heating. This property of burning plasmas may lead to thermal excursions (uncontrolled heating) or quenching (uncontrolled cooling). But even when operating at stable equilibria, system performance during transients and against disturbances could be undesirable without feedback control.

Neglecting ohmic power, which is usually small compared to the other sources in a burning plasma, and optimistically assuming that the radiation power is also negligible, at steady state ($dW/dt \equiv 0$) the energy balance (16) reduces to

$$-\frac{W}{\tau_W} + P_\alpha + P_{aux} = 0 \tag{24}$$

Taking into account that $n_\alpha, n_I << n_D, n_T$, and assuming $T_e = T_i$ and $n_D = n_T$, which implies from (21) that $n_e = n_i$ and $n = 2n_e$, we can firstly write the fusion power density in (23) as $P_f \propto \beta^2 B^4$, where $\beta \triangleq 2n_e k T_e / (B^2/(2\mu_o))$ denotes the ratio between kinetic and magnetic pressure, and secondly conclude from (24) that to operate at ignition ($P_{aux} \equiv 0 \Leftrightarrow Q \triangleq P_f/P_{aux} = \infty$) we need

$$n_e \tau_W T_e|_{IGN}^{DT} \propto \frac{T_e^2}{\langle \sigma v \rangle Q_{DT}} \tag{25}$$

This condition is usually referred to as the Lawson criterion (or as Triple Product if written in this form). The expression on the right is plotted in Fig. 12. This condition indicates that the product of confinement and pressure (density and temperature) needs to be above certain levels to achieve ignition. When compared to other fusion reactions, the DT reaction appears once again as the most promising one since it achieves the lowest minimum at the lowest temperature. Unfortunately, as we increase kinetic pressure in order to increase plasma performance (β, P_f, Q), we reach MHD stability boundaries since many of these instabilities are triggered by pressure (see Section V).

2) Burn Control: Due to the nonlinear coupled dynamics of the plasma, feedback control of the burn condition will be necessary in ITER and future fusion reactors to avoid undesirable transient performance and to respond to changes in plasma confinement, impurity content, or operation conditions that could lead to thermal excursion or quenching. Since the primary goal is to regulate the overall amount of fusion power produced by the reactor, 0D models such as (16)–(20) are appropriate for the design of controllers for tight regulation of plasma density and temperature. In order to overcome the operability limits imposed by the linearization of the burn dynamics in prior work, nonlinear techniques for burn control [59], [60] have been proposed to account for the non-local character of the dynamics and to extend the stable operating region. The controllers utilize several actuators

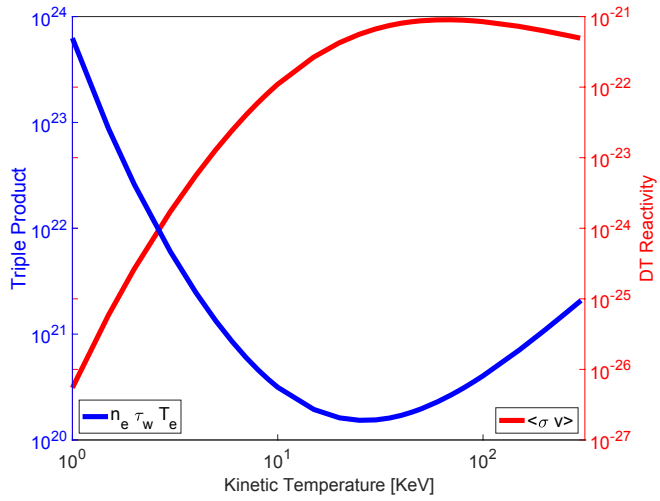

Fig. 12. Reactivity (red - right) and Triple Product (Lawson) criterion (blue - left) for a DT burning plasma.

simultaneously, using auxiliary power modulation to prevent quenching, impurity injection to stop thermal excursions by increasing radiation losses, and fueling modulation to regulate the density. Isotopic fuel tailoring [61], which requires separated actuation of the deuterium and tritium fueling systems to allow for control of the isotopic mix in the core, was exploited more recently to use the relative mix of tritium fuel in the plasma as a virtual control to cool the plasma during thermal excursions. In this way, impurity injection, and the consequent reduction in fusion power because of enhanced radiation, needs to be used only in cases where isotopic fuel tailoring is limited by severe particle recycling conditions [62]. Recycling describes the various processes that may occur when an ion exits the plasma and strikes some plasma facing component. The incident ion either immediately reflects back into the plasma or implants itself into the material. After implantation, the particle might get trapped in the material. Alternatively, the particle could randomly diffuse out of the material, re-emit into the plasma and contribute to the recycling flux. Recent experimental results in DIII-D [63] have shown the in-vessel coil system as another effective actuator for burn control. The in-vessel coils can be used to generate non-axisymmetric magnetic fields that are able to reduce the energy confinement time, becoming in this way an alternative actuation mechanism for reduction of the plasma stored energy [64]. In addition to being capable of rejecting perturbations leading to both thermal excursion and quenching, when complemented with real-time model-based optimizing schemes [65], the controllers can drive the system from one point to another during operation. Hence, the controllers can increase or decrease β, modify the fusion power, the temperature or the density, and go from a subignition ($Q < \infty$) to an ignition ($Q = \infty$) point and vice versa. Moreover, the controllers are robust against model uncertainties in the confinement times.

The ITER Organization (the organization responsible for building and operating ITER) recently realized that the plant system producing the tritium needed to fuel the ITER reactor might not be able to maintain the originally specified concentration (90% T + 10% D in the DT fueling line and 100% D in the D fueling line), particularly for long pulse operation. This fueling limitation might severely impact burn control in ITER and prevent the achievement of desired high-Q operating points. The steady-state plasma conditions for $Q = 10$ operation in ITER are studied in the density-temperature space [66]. The steady-state solution of (16)–(20) is found repeatedly over a grid of fixed n_e and T_0 values, where T_0 is the temperature on the magnetic axis of the assumed temperature profile at the moment of computing the volume-averaged quantities in (16)–(20). The unknowns are the alpha particle density fraction $f_\alpha = n_\alpha/n_e$, the external fueling rate of deuterium S_D, the external fueling rate of tritium S_T, and the impurity density fraction $f_I = n_I/n_e$. The resulting contour lines are plotted in the n_e-T_0 space in Fig. 13. This study assumes $H = 1$, $\gamma \triangleq n_T/(n_T + n_D) = 0.5$, and Neon as impurity ($Z_I = 10$). Multiple lines mark the saturation curves of the ITER actuators. The dashed-blue line marks where $P_{aux} = 0$. Below this line, the auxiliary power is negative and the results are physically meaningless. The solid-blue line denotes where $P_{aux} = 73$ MW, the maximum power expected to be available in ITER. The yellow line marks where the D injector saturates. Where the D-T injector saturates with a tritium concentration of 90%, 80%, and 70% is plotted using the solid-red, dashed-dotted-red and dotted-red lines, respectively. On the magenta line, the total plasma power, P_{total}, equals the threshold power P_{thresh} (the plasma is in H-mode (high-confinement mode - an operating mode characterized by an enhanced level of energy confinement) above this line). The green zone marks the steady-state operable space with $Q = 10$ for the given ITER plasma (tritium concentration of 90% in the DT fueling line). Here, the actuator saturation limits are not violated and the plasma is in H-mode. This operable space, which is already relatively small, shrinks as the tritium concentration decreases and vanishes when the tritium concentration in the DT fueling line drops below 60%. Even if nominal concentrations could be initially achieved, it might not be possible to keep them up for the total duration of long pulses. After about 400s of burn, the T concentration in the DT line would likely begin to drop and could go down to 80%. To add to the challenge, neither the perturbation nor the drift in the concentrations would be directly measurable without an expensive solution. This has motivated recent work towards the design of a nonlinear controller capable of overcoming unmeasurable variations of the D-T concentration expected in the fueling lines during long-pulse operation [67] by exploiting Lyapunov Redesign techniques.

VII. TOKAMAK EXCEPTION HANDLING

As discussed in the introduction, low disruptivity operation is key to maintaining integrity of the tokamak. There are multiple disturbances that can occur asynchronously including, e.g., the failure of an actuator or sensor, which can lead to plasma destabilization so that it disrupts. We label this type of disturbance an event. Some events can be handled

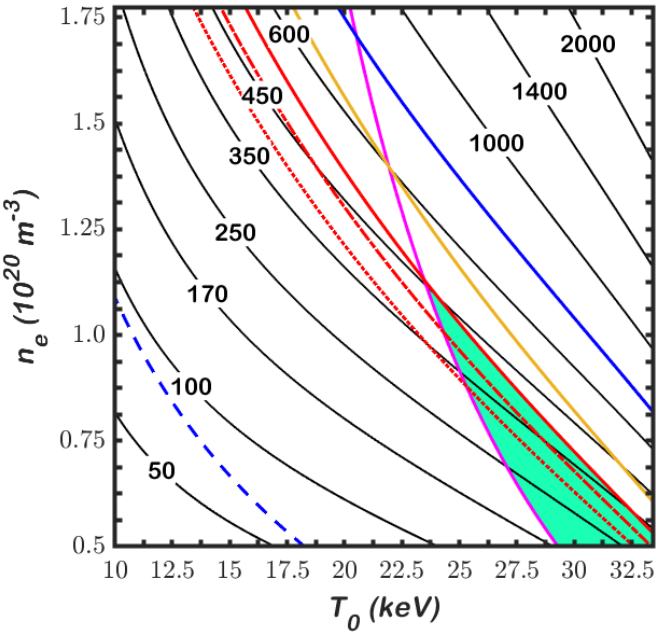

Fig. 13. Contours of constant ITER fusion power [MW] (black) for plasma with $k_D = k_T = k_\alpha = 1$ and no particle recycling. Shaded area represents Q=10 operation, bounded above by the maximum 90% tritium fueling and below by the power required for enhanced confinement (H-mode) operation.

by sufficiently robust control. Others, like the loss of a critical actuator, require a change in control approach such as switching to use of a controller that employs a different actuator or changing the control goal, e.g. to controllably terminating the discharge (i.e., without disrupting). If a response requires changing the control approach, we relabel the event as an exception.

Exception handling (EH) is a function or combination of functions in the PCS that detects such exceptions and adapts the control approach to prevent or mitigate a control degradation or failure. The exception breaks the normal flow of execution and usually executes a pre-determined handling policy. A handling policy is basically a specification of a control goal, i.e., what device operators would like to happen when a particular exception appears. The plant and the nominal plasma control should be so reliable that exceptions are rare.

Controlled termination of a tokamak discharge is not easy, especially if initiated when the plasma is at high performance (e.g., high plasma current or during the fusion-burn-phase) and even more so when control robustness has been compromised. Not all exceptions necessarily lead to controlled terminations. For example, EH can be used to optimize pulse evolution including enabling necessary changes of control schemes. Nevertheless, the risk of tokamak discharge disruptions make a well-developed exception handling capability a vital part of a tokamak control system.

Early versions of Plasma Control Systems were developed around requirements of individual control functions, such as the need to control the plasma current, the magnetic confinement configuration, or the plasma density or the heating systems. Fault or exception handling methods were added in an ad-hoc manner when deemed necessary, without a clear architectural strategy. Exceptions were typically handled on a case-by-case basis. In the simplest case, all of them were simply assigned to a single handling policy, such as switching off all heating and fueling actuators and ramping down plasma current. With hundreds of input signals and dozens of control parameters and actuators, the number of possible exceptions is enormous. In addition, proper handling of an exception is dependent on the system state (e.g., plasma or coil current levels, total energy content, etc.) when it occurs. With a multitude of potential fault sources and many variations in plasma dynamics, the decision logic can become very complex. Developing this logic organically leads to an increasingly complex system with too finely detailed states, poor choices in exception definition and even illogical exception responses [11]. Instead, exception handling should be designed systematically, based on knowledge of possible fault sources and their impact.

A. *Defining the set of exceptions*

The first step in defining an automated system is to identify all exceptions that must be handled by the PCS. This begins by determining which events can be handled with sufficiently robust control and which must be treated as exceptions. This process requires participation of both physics operators (responsible for operation of the device) and control engineers, who are best able to understand what can be handled via standard disturbance rejection. Next, physics operators must define a handling policy for each exception, i.e., how the control goal should change to effectively prevent or mitigate any negative consequences of the exception.

1) Basic tokamak exception handling: In Fig. 14, an example is given of active instability control using a single actuator. Preferred operation is in the ideal control zone, where even large actuator perturbations do not affect stabilizability. Improving fusion performance often requires relying on control robustness at a less stable operating point. An actuator fault could result in a transition back to a stabilized recovery state, if properly handled by EH, or a loss of control, requiring a hard (uncontrolled) termination of the discharge. If in a recovery state, the EH system can decide to recover or to terminate the discharge.

This example (and all other desired handling of tokamak exceptions) can be represented by a finite state diagram (Fig. 15) that consists of a number of characteristic states - normal (ideal) control, robust control, recovery state, controlled termination and hard termination. Hard termination is the application of measures to mitigate the impact of, rather than prevent, a disruption. Mitigation measures can reduce, but usually not eliminate, the impact of the exception on the device. Their use should be minimized by preventing, if possible, the disruption from occurring. Each transition between states in Fig. 15 represents an exception handling policy. The transition goal state depends on the reason for the transition - often an actuator or control fault - and the initial system state.

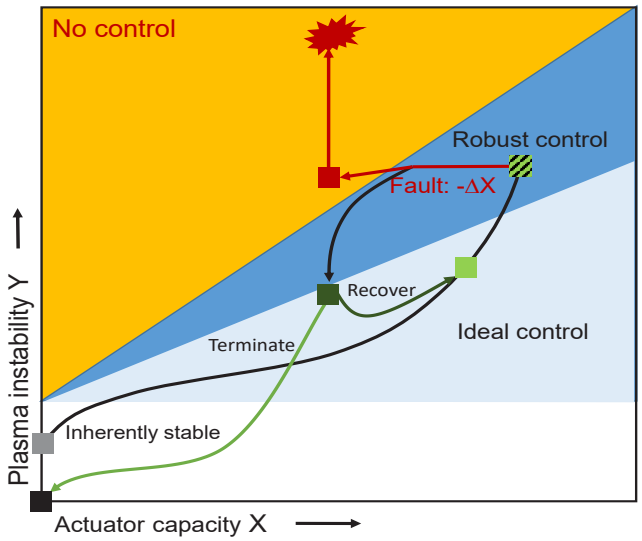

Fig. 14. Control of a plasma instability with growth rate defined by parameter Y, using an actuator X. By means of sufficiently robust active control, it is possible to operate at high Y (cross-hatched symbol) to optimize fusion performance. An actuator fault could cause the instability to be uncontrollable (red symbol) and result in disruption. Exception handling should ensure that such events are detected and bring the plasma and plant into a more stable lower performance state (dark green symbol), after which recovery of operation or termination (reducing X and Y to zero) is possible.

Finite state machines have been implemented in existing plasma control systems in efforts to improve disruption prevention [38], [68] and also to better optimize actuator management (i.e. manage requests from different control functions for the same set of actuators) [40], but these efforts have not yet reached the level of sophistication required for devices like ITER.

2) Determining required exceptions and priorities: Using Failure Mode Effect Analysis (FMEA), a complete inventory is made of possible exceptions (failure modes) that could lead to undesirable outcomes. The FMEA also determines the likelihood of occurrence of the failure mode (per plasma discharge), the severity or impact of the failure, and the difficulty to detect it, which in combination gives a risk value due to the exception (i.e. *occurrence* $\times$ *severity* $\times$ *undetectability*). In an alternative approach, a Fault Tree Analysis (FTA) works backward from an undesirable outcome to identify potential failure modes. This analysis has the advantage over the FMEA of allowing the process that leads to the event to be evaluated, as opposed to looking at the failure mode in isolation. Both methods allow prioritization of faults based on exception consequences. Figure 16 shows a basic tree of characteristic events that can lead to a plasma disruption. Many possible exception sources on the left (human error, computing error, transient event, sensor or actuator fault), can lead to a sequence of events that eventually ends with a disruption. For a plant as complex as a tokamak, this collection of exception sources leads to a large list of exceptions.

B. Automated exception handling approach

The obvious ”algorithm” for automating exception handling is that an exception, if it occurs, must be first detected

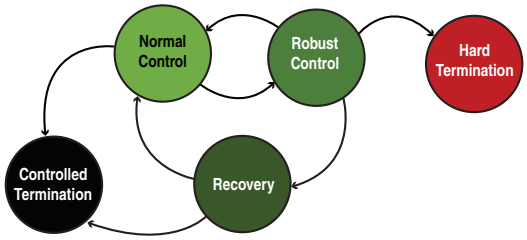

Fig. 15. A number of characteristic states can be identified from the example shown in the previous figures, as well as the transitions between them, resulting in the following basic finite state-diagram. The transitions between are the handling policies. However, this only represent one typical control function, and there exist many, that all again interact with each other, creating possible a very complicate state-diagram, with numerous possible transitions, or exceptions.

(or predicted in advance if possible), then an alternate control must be activated. A number of technologies exist for automated detection including, e.g., simple threshold comparison of a relevant signal, statistical classification algorithms, and neural networks, the latter two of which are able to operate on multiple signals or information sources. Ultimately, all methods derive a ”decision variable” whose value is used to make the decision about whether to declare an exception. A threshold is chosen so that the exception is declared when the decision variable’s value is greater than the threshold. One method for choosing this threshold uses the so-called ROC (receiver operating characteristic) curve (Fig. 17). The key metrics for detection/prediction processes are the probability of correct detection (P_d) and probability of false alarm (P_{fa}). The threshold is chosen so that a satisfactory trade-off is achieved between detection of the true exceptions (P_d) and spurious declaration of exception when none exists (P_{fa}).

Once an exception is declared, control must switch to execution of a predetermined handling policy, i.e., a specified new control goal (typically instantiated as a set of control reference signals, which implicitly include, of course, the identity of the variable(s) chosen to be controlled). Executing the policy may or may not require the use of a different set of controllers.

The effectiveness of a handling policy is often compromised by a slow response of the plasma or actuators. To overcome this, forecasting of future events can make it possible to still provide timely response. Forecasting functions (open-loop system models), whose predicted signal values are used to evaluate likelihood of future exceptions, can be included in the PCS. Methods used can be as simple as extrapolation using a linearized response model or can be based on faster-than-real-time simulation of future plasma evolution.

Obviously most attention on forecasting is focused on disruptions. Simply detecting an ongoing disruption enables triggering of mitigating measures for some of its consequences, but not all [69]. For example, mitigation of heat loads due to the fast quench of thermal energy during disruptions (on order of a few ms) is not possible. The standard mitigation method of injecting large amounts of particles into the tokamak takes at least several tens of milliseconds. Thus considerable efforts have been dedicated to providing

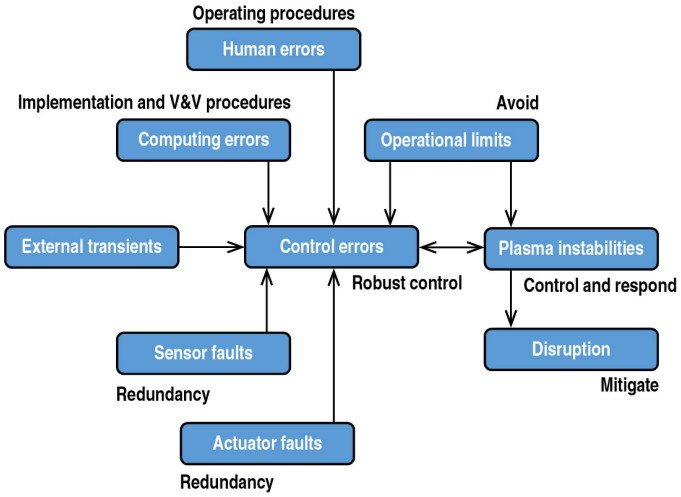

Fig. 16. A basic event tree analysis of a tokamak discharge disruption. For a single disruptive outcome, there are multiple potential causes (either alone or in combination) including plasma instabilities, operational limits, control errors, actuator and sensor faults, and external transients. Computation or human error can also lead to disruption. The many-to-many relationships result in a complex set of potential event paths leading to disruption. This diagram can be compared with an actual root-cause analysis for disruptions in the JET tokamak [70]. Next to the boxes defining event types, basic techniques to mitigate the events are shown.

advance prediction of thermal quench in plasmas [10].

Prediction of disruptions can be achieved by detecting specific instabilities that grow in the plasma prior to disruption. Such techniques are reasonably successful but generally not good enough to predict disruptions in devices such as ITER which, because of limited tolerance to the impact of thermal quenches, requires them to have a very high success rate [69]. In recent years, more advanced methods have aimed to predict disruptions using neural networks. These neural networks have been trained on a large set of example plasma discharges, to distinguish between those that disrupt and those that do not. The disadvantage of these methods is that they focus purely on the plasma stability and not, for example, on the detection of incipient actuator and sensor faults or control errors, which are often the root cause of the plasma destabilization. The PCS must monitor all of these potential sources of disruption.

In addition to disruptions, the PCS may be able to forecast impending threats if continuing as scheduled. For example, a control scheme may be sufficiently robust in the current plasma state. However if, for example, plasma pressure is increased further, the available set of sensors and actuators may not be capable of supporting the required control robustness. So-called hazard-functions can be determined in real-time based not only the stability of the plasma, but also the general state of the plasma control [71]. Hazard-functions provide estimated future event probabilities as a function of time, allowing the control system to act if the probability of a high-risk event is large but the event has not yet taken place. This approach provides more complete coverage of detection of the root causes of disruptions.

C. Managing complexity

Even a concise definition of exceptions using, e.g., FMEA and FTA, will result in a very large number of them. Together with the many plasma and plant state-specific responses , this can result in an explosion of possible exception handling paths. It is important to contain the complexity of PCS EH or it may become impossible to validate its design or to commission it.

The only feasible method for limiting the number of exceptions is to ignore faults that do not lead to important consequences if not handled in real-time. On the other hand, exception priorities defined by FMEA and FTA can be used to manage their handling. For example, exceptions do not generally occur in isolation, since the modified plasma state resulting from an initial exception will often create conditions in which other exceptions occur. In fact, multiple exceptions can often occur closely together in time. If one exception follows another having lower priority, response to the later exception may need to override the earlier triggered handling policy. The handling policies of the two exceptions could be contradictory. The first exception could request to turn-off an actuator that is required to handle the later, more important exception. Delay in re-activation of this actuator could affect handling of the later higher-priority exception. Some guidance for how to manage conflicting exception responses through priorities is available. For example, [72] and the references therein discuss prioritized execution in hard real-time systems (but focus on faults in the computational process). There is also experience with fault handling in nuclear power plants that may be relevant (e.g., [73] and references therein). However, further research on prioritized execution is needed for application in tokamaks.

One can also attempt to limit the number of possible handling policies. In tokamak research, the stability and characteristics of discharge terminations are studied [74]. The aim is often to develop a single policy robust enough to be used for discharge termination in response to a large number of events. For simple plasma discharges, this may well be possible. However, controlled termination of a burning plasma - the main target of ITER operation - is complex, and variations in handling policy are needed depending on the plasma state or control capabilities. Hence, the control system will be required to choose from a list of termination policy variants.

Complexity can also be reduced by defining intermediate handling policies (goals) such that a sequence of such policies accomplishes an overall goal. For example, if the overall goal is to terminate the plasma discharge, there is likely to exist an intermediate goal to first bring the plasma to a more stable target state. Although this is only a one-step example, the value in the approach is the ability to define for each exception a sequence of steps between intermediate goal states, with a smaller set of potential states at each step, which at the end reaches the final termination goal.

This approach does not actually reduce the number of paths that must be taken between the overall set of excep-

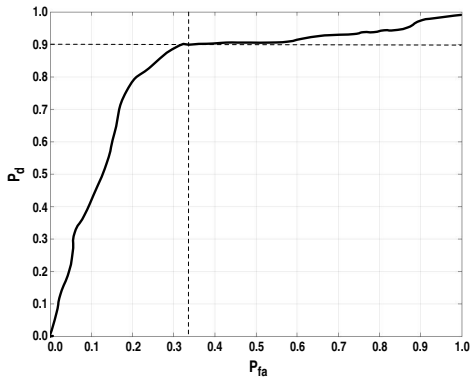

Fig. 17. Illustration of an ROC curve, which plots calculated P_d and P_{fa} values for many possible thresholds. A point on this curve can be used to choose a threshold for the decision variable .

tions and the termination goal, but it does allow re-use of previously programmed handling policies. This means that construction of a handling policy for a new exception is not required to define the entire evolution to termination from the plasma state at the time of exception. Instead, it can choose from already defined intermediate "handling" states the one that is most easily achieved from the beginning state. In fact, as the exception handling system of the JET tokamak was being built over time, it was found that the system naturally evolved into this pattern.

D. Aspects of control design for EH

Many requirements for controllers used to execute handling policies are similar to those of nominal control, but there are some important additional constraints. Smoothly transitioning to the new control is critical to prevent triggering of a secondary exception while handling the first. Robustness of the new control is paramount, even at the expense of performance, since inadequate achievement of the control goal(s) may lead to device damage. Robustness can also serve to reduce control system complexity (and therefore risk) by enabling one handling policy to service multiple exceptions.

In the traditional approach, a handling policy would define reference signals which, if followed, would transition the system into a "safe" state. It would also define the controllers to be used to force the system to track those references. However, the most advanced handling policy would be one that is not prescribed in advance, but is optimally chosen by the control system. Model-based predictive control (MPC) could determine, based a set of constraints and faster than real-time predictive modeling of the system, what the optimum transition is between the initial system state when the exception occurs and a specified stable target state at the end of the MPC prediction horizon. Using the example of discharge termination, instead of following a predefined set of reference signals an MPC can choose the path that it follows to achieve the target end state. A mixture of hard and soft state constraints on the MPC can be used to avoid potential sources of instability in addition to dealing with the usual actuator limitations. However, if it is necessary to also make updates to control methods used during this evolution, a significant extension of traditional MPC would be required.

Since requirements for nominal control are usually well defined, validation of a controller's capabilities prior to operational use is straightforward. However, validation of the suggested MPC algorithm's execution of exception response or even defining its prerequisite control requirements may be challenging. Specification of control metrics such as response time, settling time, tracking error, etc. are well-understood, but a similar metric for "goal achievement" must still be defined to enable quantitative comparison with alternative handling policies or with requirement specifications.

REFERENCES

[1] [Online]. Available: http://www.iter.org

[2] Pironti and Walker, "Control of tokamak plasmas: introduction to a special section," *IEEE Control Systems Magazine*, vol. 25, no. 5, pp. 24–29, Oct 2005.

[3] ——, "Fusion, tokamaks, and plasma control: an introduction and tutorial," *IEEE Control Systems Magazine*, vol. 25, no. 5, pp. 30–43, Oct 2005.

[4] Walker *et al.*, "Emerging applications in tokamak plasma control," *IEEE Control Systems Magazine*, vol. 26, no. 2, pp. 35–63, April 2006.

[5] [Online]. Available: https://www.iter.org/sci/Fusion

[6] [Online]. Available: http://www.ga.com/diii-d

[7] Artsimovich and Shafranov, "Tokamak with non-round section of the plasma loop," *Soviet Phys. - JETP Letters 13.72*, 1972.

[8] Freidberg, *Ideal MHD*. Cambridge University Press, 2014, pp. i–iv.

[9] Hender *et al.*, "Chapter 3: MHD stability, operational limits and disruptions," *Nuclear Fusion*, vol. 47, no. 6, pp. S128–S202, 2007.

[10] Strait, Barr, Baruzzo *et al.*, "Progress in disruption prevention for ITER," *Nuclear Fusion*, vol. 59, no. 11, p. 112012, jun 2019.

[11] Humphreys *et al.*, "Novel aspects of plasma control in ITER," *Phys. of Plasmas*, vol. 22, no. 2, p. 021806, Feb 2015.

[12] Ariola and Pironti, *Magnetic Control of Tokamak Plasmas*, ser. Advances in Industrial Control. Springer International Publishing, 2016.

[13] Skogestad and Postlethwaite, *Multivariable Feedback Control*. John Wiley & Sons Ltd., 2005.

[14] Albanese, Ambrosino, and Mattei, "CREATE-NL+: A robust control-oriented free boundary dynamic plasma equilibrium solver," *Fusion Eng. and Design*, vol. 96-97, pp. 664–667, oct 2015.

[15] Albanese *et al.*, "Design, implementation and test of the XSC extreme shape controller in JET," *Fusion Eng. and Design*, vol. 74, no. 1-4, pp. 627–632, nov 2005.

[16] Anand *et al.*, "A novel plasma position and shape controller for advanced configuration development on the TCV tokamak," *Nuclear Fusion*, vol. 57, no. 12, p. 126026, dec 2017.

[17] Albanese *et al.*, "A MIMO architecture for integrated control of plasma shape and flux expansion for the EAST tokamak," in *2016 IEEE Conference on Control Applications (CCA)*. IEEE, sep 2016, pp. 611–616.

[18] Gerkšič *et al.*, "Model predictive control of ITER plasma current and shape using singular-value decomposition," *Fusion Eng. and Design*, vol. 129, pp. 158–163, apr 2018.

[19] Ariola *et al.*, "A Modern Plasma Controller Tested on the TCV Tokamak," *Fusion Technology*, vol. 36, no. 2, pp. 126–138, sep 1999.

[20] Nouailletas, Nardon, and Brémond, "Robust Vertical Plasma Stabilization of the future tungsten divertor configuration of Tore Supra," *IFAC Proceedings Volumes*, vol. 47, no. 3, pp. 1349–1354, 2014.

[21] Ferrara, Hutchinson, and Wolfe, "State Reconstruction and Noise Reduction by Kalman Filter in the Vertical Position Control on Alcator C-Mod," *Fusion Science and Technology*, vol. 56, no. 4, pp. 1476–1488, nov 2009.

[22] Hyatt *et al.*, "Designing, constructing and using Plasma Control System algorithms on DIII-D," in *2013 IEEE 25th Symp. on Fusion Eng.* IEEE, jun 2013, pp. 1–6.

[23] Hahn *et al.*, "Progress and improvement of KSTAR plasma control using model-based control simulators," *Fusion Eng. and Design*, vol. 89, no. 5, pp. 542–547, may 2014.

[24] Nouailletas *et al.*, "The WEST plasma control system: Integration, commissioning and operation on first experimental campaigns," *Fusion Eng. and Design*, vol. 146, pp. 999–1002, sep 2019.

[25] Kolemen *et al.*, "Strike point control for the National Spherical Torus Experiment (NSTX)," *Nuclear Fusion*, vol. 50, no. 10, p. 105010, oct 2010.

[26] Zohm, *Magnetohydrodynamic Stability of Tokamaks*. Weinheim, Germany: Wiley-VCH Verlag GmbH & Co. KGaA, dec 2014.

[27] Lanctot *et al.*, "Error field optimization in DIII-D using extremum seeking control," *Nuclear Fusion*, vol. 56, no. 7, p. 076003, jul 2016.

[28] Dalessio *et al.*, "Model-based Robust Control of Resistive Wall Modes via μ-synthesis," *Fusion Science and Technology*, vol. 55, no. 2, pp. 163–179, 2009.

[29] Katsuro-Hopkins, Bialek, Maurer, and Navratil, "Enhanced ITER resistive wall mode feedback performance using optimal control techniques," *Nuclear Fusion*, vol. 47, no. 9, pp. 1157–1165, sep 2007.

[30] Chapman *et al.*, "Sawtooth control using electron cyclotron current drive in ITER demonstration plasmas in DIII-D," *Nuclear Fusion*, vol. 52, no. 6, p. 63006, 2012.

[31] Lennholm *et al.*, "Feedback control of the sawtooth period through real time control of the ion cyclotron resonance frequency," *Nuclear Fusion*, vol. 51, no. 7, p. 073032, jul 2011.

[32] Goodman, Felici, Sauter, and Graves, "Sawtooth pacing by real-time auxiliary power control in a tokamak plasma," *Physical Review Letters*, vol. 106, no. 24, 2011.

[33] Rapson *et al.*, "Amplitude based feedback control for NTM stabilisation at ASDEX Upgrade," *Fusion Eng. and Design*, vol. 89, no. 5, pp. 568–571, 2014.

[34] Kolemen *et al.*, "State-of-the-art neoclassical tearing mode control in DIII-D using real-time steerable electron cyclotron current drive launchers," *Nuclear Fusion*, vol. 54, no. 7, p. 073020, jul 2014.

[35] Hennen *et al.*, "Real-time control of tearing modes using a line-of-sight electron cyclotron emission diagnostic," *Plasma Physics and Controlled Fusion*, vol. 52, no. 10, p. 104006, 2010.

[36] Felici *et al.*, "Integrated real-time control of MHD instabilities using multi-beam ECRH/ECCD systems on TCV," *Nuclear Fusion*, vol. 52, no. 7, p. 074001, jul 2012.

[37] Maljaars and Felici, "Actuator allocation for integrated control in tokamaks: architectural design and a mixed-integer programming algorithm," *Fusion Eng. and Design*, oct 2017.

[38] Eidietis *et al.*, "Implementing a finite-state off-normal and fault response system for disruption avoidance in tokamaks," *Nuclear Fusion*, vol. 58, no. 5, p. 056023, may 2018.

[39] Vu *et al.*, "Tokamak-agnostic actuator management for multi-task integrated control with application to TCV and ITER," *Fusion Eng. and Design*, vol. 147, p. 111260, oct 2019.

[40] Blanken *et al.*, "Real-time plasma state monitoring and supervisory control on TCV," *Nuclear Fusion*, vol. 59, no. 2, p. 026017, jan 2019.

[41] Kong *et al.*, "Control of neoclassical tearing modes and integrated multi-actuator plasma control on TCV," *Nuclear Fusion*, vol. 59, no. 7, p. 076035, jul 2019.

[42] Pajares *et al.*, "Integrated current profile, normalized beta and NTM control in DIII-D," *Fusion Eng. and Design*, vol. 146, pp. 559–562, sep 2019.

[43] Peeters, "The Bootstrap Current and Its Consequences," *Plasma Phys. and Control. Fusion*, vol. 42, pp. B231–B242, 2000.

[44] St. John, "Equations and associated definitions used in ONETWO." [Online]. Available: http://fusion.gat.com/THEORY/onetwo/

[45] Hinton and Hazeltine, "Theory of Plasma Transport in Toroidal Confinement Systems," *Rev. of Modern Physics*, vol. 48, no. 2, pp. 239–308, 1976.

[46] Ou *et al.*, "Towards Model-based Current Profile Control at DIII-D," *Fusion Eng. and Design*, vol. 82, pp. 1153–1160, 2007.

[47] Witrant *et al.*, "A Control-oriented model of the Current Profile in Tokamak Plasma," *Plasma Phys. and Controlled Fusion*, vol. 49, pp. 1075–1105, 2007.

[48] Felici *et al.*, "Real-time physics-model-based simulation of the current density profile in tokamak plasmas," *Nuclear Fusion*, vol. 51, no. 083052, 2011.

[49] Xu *et al.*, "Ramp-Up Phase Current Profile Control of Tokamak Plasmas via Nonlinear Programming," *IEEE Trans. Plasma Science*, vol. 38, no. 2, pp. 163–173, February 2010.

[50] Felici and Sauter, "Non-linear model-based optimization of actuator trajectories for tokamak plasma profile control," *Plasma Phys. and Controlled Fusion*, vol. 54, no. 025002, 2012.

[51] Wehner *et al.*, "Optimal Current Profile Control for Enhanced Repeatability of L-mode and H-mode Discharges in DIII-D," *Fusion Eng. and Design*, vol. 123, pp. 513–517, 2017.

[52] Ou *et al.*, "Receding-Horizon Optimal Control of the Current Profile Evolution During the Ramp-up Phase of a Tokamak Discharge," *Control Eng. Practice*, vol. 19, pp. 22–31, 2011.

[53] Maljaars *et al.*, "Control of the tokamak safety factor profile with time-varying constraints using MPC," *Nuclear Fusion*, vol. 55, no. 2, p. 023001, 2015.

[54] Wehner *et al.*, "Predictive control of the tokamak q profile to facilitate reproducibility of high-q_{min} steady-state scenarios at DIII-D," in *Proc. of IEEE Conf. on Control Appl.*, Buenos Aires, Argentina, Sep. 19-22 2016, pp. 629–634.

[55] Dalessio *et al.*, "Model-based Control of the Resistive Wall Mode in DIII-D: A Comparison Study," *Fusion Eng. and Design*, vol. 84, pp. 641–645, 2009.

[56] Wehner, Barton, and Schuster, "Toroidal Rotation Profile Control for the DIII-D Tokamak," in *Proc. of 2015 American Control Conf.*, Chicago, IL, USA, July 1-3 2015, pp. 3664–3669.

[57] Wehner, Barton, and Schuster, "Combined rotation profile and plasma stored energy control for the DIII-D tokamak via MPC," in *Proc. of 2017 American Control Conf.*, Seattle, WA, USA, May 24-26 2017, pp. 4872–4877.

[58] N. A. Uckan, "Confinement capability of ITER-EDA design," *Proc. of 15th IEEE/NPSS Symp. on Fusion Eng.*, vol. 1, pp. 183–186, 1993.

[59] Schuster, Krstic, and Tynan, "Nonlinear Lyapunov-Based Burn Control in Fusion Reactors," *Fusion Eng. and Design*, vol. 63-64, pp. 569–575, 2002.

[60] ——, "Burn Control in Fusion Reactors via Nonlinear Stabilization Techniques," *Fusion Science and Technology*, vol. 43, no. 1, pp. 18–37, January 2003.

[61] Gouge, Houlberg, Attenberger, and Milora, "Fuel source isotopic tailoring and its impact on ITER design, operation and safety," *Fusion Technology*, vol. 28, pp. 1–18, 1995.

[62] Boyer and Schuster, "Nonlinear burn condition control in tokamaks using isotopic fuel tailoring," *Nuclear Fusion*, vol. 55, no. 8, p. 083021, 2015.

[63] Hawryluk, Eidietis, Grierson, and Hyatt, "Control of plasma stored energy for burn control using DIII-D in-vessel coils," *Nuclear Fusion*, vol. 55, p. 053001 (9pp), 2015.

[64] Pajares and Schuster, "Nonlinear Burn Control Using In-vessel Coils and Isotopic Fueling in ITER," *Fusion Eng. and Design*, vol. 123, pp. 607–611, 2017.

[65] Boyer and Schuster, "Nonlinear control and online optimization of the burn condition in ITER via heating, isotopic fueling and impurity injection," *Plasma Phys. and Controlled Fusion*, vol. 56, no. 10, p. 104004, 2014.

[66] Graber and Schuster, "Tritium-concentration requirements in the fueling lines for high-q operation in iter," in *Proc. 46th European Physical Society Conf. on Plasma Physics*, Milan, Italy, 2019.

[67] Pajares and Schuster, "Robust nonlinear burn control in ITER to handle uncertainties in the fuel-line concentrations," *Nuclear Fusion*, vol. 59, no. 9, p. 096023, jul 2019.

[68] Maraschek *et al.*, "Path-oriented early reaction to approaching disruptions in ASDEX upgrade and TCV in view of the future needs for ITER and DEMO," *Plasma Physics and Controlled Fusion*, vol. 60, no. 1, p. 014047, nov 2017.

[69] De Vries *et al.*, "Requirements for triggering the iter disruption mitigation system," *Fusion Science and Technology*, vol. 69, no. 2, pp. 471–484, 2016. [Online]. Available: https://doi.org/10.13182/FST15-176

[70] ——, "Survey of disruption causes at JET," *Nuclear Fusion*, vol. 51, no. 5, p. 053018, apr 2011.

[71] Olofsson, Humphreys, and Haye, "Event hazard function learning and survival analysis for tearing mode onset characterization," *Plasma Physics and Controlled Fusion*, vol. 60, no. 8, p. 084002, jun 2018.

[72] Punnekkat, "Schedulability Analysis for Fault Tolerant Real-Time Systems," *Dissertation, University of York*, June 1997.

[73] Jianping Ma, "Applications of Fault Diagnosis in Nuclear Power Plants: An Introductory Survey," *Proc. of 7th IFAC Symp. on Fault Detection, Supervision and Safety of Technical Processes, Barcelona, Spain,*, June 30 - July 3 2009.

[74] De Vries *et al.*, "Multi-machine analysis of termination scenarios with comparison to simulations of controlled shutdown of ITER discharges," *Nuclear Fusion*, vol. 58, no. 2, p. 026019, Dec 2017.